Dispersal and Population Connectivity in the Deep North Atlantic Estimated from Physical Transport Processes.

Ron J. Etter*
Biology Department
University of Massachusetts Boston,
Boston 02125 USA
E-mail address: ron.etter@umb.edu
Corresponding Author

Amy S. Bower
Department of Physical Oceanography
Woods Hole Oceanographic Institution
Woods Hole, Massachusetts, 02543, USA
E-mail address: abower@whoi.edu

* Both authors contributed equally to this work

Running title: Dispersal and connectivity in the deep Atlantic

Abstract

Little is known about how larvae disperse in deep ocean currents despite how critical estimates of population connectivity are for ecology, evolution and conservation. Estimates of connectivity can provide important insights about the mechanisms that shape patterns of genetic variation. Strong population genetic divergence above and below about 3000m has been documented for multiple protobranch bivalves in the western North Atlantic. One possible explanation for this congruent divergence is that the Deep Western Boundary Current (DWBC), which flows southwestward along the slope in this region, entrains larvae and impedes dispersal between the upper/middle slope and the lower slope or abyss. We used Lagrangian particle trajectories based on an eddy-resolving ocean general circulation model (specifically FLAME - Family of Linked Atlantic Model Experiments) to estimate the nature and scale of dispersal of passive larvae released near the sea floor at 4 depths across the continental slope (1500, 2000, 2500 and 3200 m) in the western North Atlantic and to test the potential role of the DWBC in explaining patterns of genetic variation on the continental margin. Passive particles released into the model DWBC followed highly complex trajectories that led to both onshore and offshore transport. Transport averaged about 1 km d^{-1} with dispersal kernels skewed strongly right indicating that some larvae dispersed much greater distances. Offshore transport was more likely than onshore and, despite a prevailing southwestward flow, some particles drifted north and east. Dispersal trajectories and estimates of population connectivity suggested that the DWBC is unlikely to prevent dispersal among depths, in part because of strong cross-slope forces

induced by interactions between the DWBC and the deeper flows of the Gulf Stream. The strong genetic divergence we find in this region of the Northwest Atlantic is therefore likely driven by larval behaviors and/or mortality that limit dispersal, or local selective processes (both pre and post-settlement) that limit recruitment of immigrants from some depths.

Keywords: Dispersal, population connectivity, circulation model, North Atlantic, protobranch bivalve, deep-sea

1. Introduction

Understanding how populations are connected through dispersal is of fundamental importance in ecology, evolution, conservation and management, and will play a crucial role in predicting how organisms might respond to contemporary anthropogenic stresses. From an evolutionary perspective, dispersal influences gene flow among populations, which in turn affects genetic diversity, phylogeographic patterns, adaptation to local selective pressures, and ultimately the likelihood of speciation (reviewed in Nosil, 2012). At an ecological scale, dispersal can influence demographic processes (Roughgarden et al., 1985), source-sink dynamics (Holt, 1985), metapopulation (Hanski ,1999) and metacommunity persistence (Leibold et al., 2004), the maintenance of biodiversity (Mouquet and Loreau, 2003; Hubbell 2001), the spread of invasive species (Neubert and Caswell, 2000; Byers and Pringle, 2006; Caswell et al., 2011) and play a vital role in management and conservation (Palumbi, 2003; Botsford et al., 2003; 2009; Gaines et al.,

2003; 2010). Connectivity links dynamics at different scales and integrates local heterogeneity affecting regional-scale dynamics and long-term persistence. Quantifying the scale over which populations are connected is vital to understand the relative importance of various ecological processes, identify the appropriate scales of environmental influence in driving population dynamics and determine how local communities might respond to environmental change.

The extent to which populations are connected is determined by the scale, intensity, direction and frequency of dispersal among populations as well as post-settlement processes that influence the fitness of recruits. For many sessile marine invertebrates, dispersal occurs during the larval stage. Larvae (or gametes) are released into the water column where they are dispersed by the currents due to both advective and diffusive processes. The speed, variability and direction of the currents have a strong effect on where larvae move, especially if they exhibit little behavior and disperse essentially as passive particles. However, the interaction between larval behavior and physical transport processes (Paris et al., 2007; North et al., 2008; Sakina-Dorothée et al., 2010; Morgan, 2014) as well as environmental heterogeneity in productivity, local fecundity and larval mortality (White et al., 2014) can profoundly influence the patterns and magnitude of connectivity among populations. Post-settlement processes can also alter patterns of connectivity if recruits do not survive to reproduce or have reduced fitness. Connectivity thus represents the integration of both biological and physical processes and involves complex interactions between benthic and pelagic forces.

Measuring connectivity in marine organisms with small propagules that drift for various lengths of time in the ocean is extremely difficult. Although the length of time larvae

drift in ocean currents has been estimated, how that translates to distance and direction traveled and thus connectivity among populations is not well understood. Because of its obvious importance in ecology, evolution and conservation, a number of techniques have been developed to estimate dispersal based on a variety of complementary approaches including larval ecology, hydrographic models, coupled bio-physical models and empirical estimates based on genetics and geochemistry (reviewed in Levin, 2006; Thorrold et al., 2007; Cowen and Sponaugle, 2009; Lowe and Allendorf, 2010; Leis et al., 2011; Kool et al., 2013). Each technique has inherent advantages and disadvantages such that a combined approach, when possible, provides a more accurate estimate of connectivity and a more complete understanding of the forces that shape patterns of connectivity (Levin, 2006; Lowe and Allendorf, 2010; Leis et al., 2011).

While considerable advances have been made in estimating dispersal in shallow-water ecosystems (e.g. Kinlan and Gaines, 2003; Bradbury et al., 2008; Shanks, 2009; Selkoe and Toonen, 2011; López-Duarte et al., 2012; Riginos et al., 2014), much less is known about dispersal in the deep ocean, except perhaps around hydrothermal vents (e.g. Marsh et al., 2001; Mullineaux et al., 2002; 2010; 2013; Adams and Mullineaux, 2008; McGillicuddy et al., 2010). Recent estimates of the scale of dispersal in deep-sea organisms based on Planktonic Larval Duration (PLDs – e.g. Young et al., 2012) or genetic patterns of isolation by distance (Baco et al., 2015) suggest larvae can disperse 100s of km and are quite similar to shallow-water organisms in dispersal distance, despite lower temperatures that likely extend PLDs (e.g. O'Connor et al., 2007; Peck et al., 2007; Kelley and Eernisse, 2007) and weaker current velocities typically associated with

increasing depth. In the deep sea, few have estimated dispersal based on physical processes (e.g. Yearsley and Sigwart, 2011; Young et al., 2012; Sala et al., 2013) and rarely have the predictions from physical transport models and/or PLDs been compared to inferences derived from patterns of genetic variation (e.g. Henry et al., 2014). Such a combined approach provides a powerful framework to test the validity of various hypotheses and provides a more complete understanding of the potential explanations for observed patterns of genetic variation (e.g. Sotka et al., 2004; Baums et al., 2006; Galindo et al., 2006; 2010; Weersing and Toonen, 2009; White et al., 2010; Alberto et al., 2011; Sunday et al., 2014). Here we use simulated Lagrangian particle trajectories based on an eddy-resolving ocean general circulation model (specifically FLAME - Family of Linked Atlantic Model Experiments) to estimate the nature and scale of dispersal at bathyal depths in the western North Atlantic and to test the potential role of the Deep Western Boundary Current (DWBC) in explaining patterns of genetic variation on the continental margin.

In particular, we test the hypothesis that the strong genetic divergence at bathyal depths in the western North Atlantic might be due to the DWBC impeding gene flow between upper and lower bathyal depths. Population genetic analyses of protobranch bivalves have repeatedly indicated strong genetic breaks along depth gradients in the western North Atlantic such that populations above and below approximately 3000m are highly divergent (Etter et al., 2005; Zardus et al., 2006; Jennings et al., 2013; Glazier and Etter, 2014). Populations separated by as little as 40km distance and 100m depth exhibited pronounced divergence at multiple loci (see Fig. 1). The strong divergence at such small scales is very surprising because dispersal over that distance is likely within the dispersal

147 window of their lecithotrophic larvae (Zardus, 2002; Scheltema and Williams, 2009) and
148 no obvious topographic features exist in this region that would impede gene flow.

149 The present day DWBC flows equatorward along the continental slope between 700 –
150 4000 m (Fig 2) with mean flows of 5-10 cm s^{-1} (Pickart and Watts, 1990; Toole et al.,
151 2011). The genetic break occurs within the DWBC, so one possible explanation for the
152 observed divergence is that the relatively strong mean southwestward flow of the DWBC
153 entrains passively (or weakly swimming) dispersing demersal larvae advecting them
154 equatorward, preventing cross slope dispersal between the upper/middle slope and the
155 lower slope or abyss. Despite the relatively strong mean flows oriented along the
156 isobaths, neutrally buoyant free-drifting floats released at depth and Lagrangian
157 simulations of particle trajectories in the DWBC suggest that circulation is highly
158 complex and departs considerably from time-averaged mean southwestward flow (Bower
159 and Hunt, 2000a; 2000b; Bower et al. 2009; 2011; 2013; Lozier et al. 2013). Both
160 empirical and simulated trajectories indicate considerable mesoscale variability with a
161 high potential of cross-slope movement (i.e. between depth regimes), especially where
162 the DWBC interacts with the Gulf Stream and its associated eddies. The highly complex
163 mesoscale flows and the high probability of floats and simulated particles to move
164 across-slope raises questions about whether the DWBC impedes larval exchange between
165 upper and lower bathyal populations. To test the hypothesis that connectivity between
166 populations from upper and lower bathyal depths might be precluded by the DWBC, we
167 estimated dispersal trajectories of simulated passive larvae (neutrally buoyant particles)
168 released along a depth gradient adjacent to our genetic samples in the western North
169 Atlantic (Fig. 1). Specifically, we examined whether particles would move across slope

and the distance they moved given certain PLDs.

2. Methods

2.1 Physical Transport Model

The ocean general circulation model used in this analysis to simulate particle trajectories is the highest resolution member of the Family of Linked Atlantic Modeling Experiments (FLAME) (Böning et al., 2006; Biastoch et al., 2008). This model uses a primitive equation, z-coordinate framework (Pacanowski, 1996) that includes isopycnal mixing, biharmonic friction and a bottom boundary layer parameterization for temperature and salinity (Beckmann and Döscher, 1997). In the vertical, the model domain is divided into 45 levels whose spacing increases from 10 m at the surface to a maximum of 250 m at the deepest levels. The ETOPO5 digital bathymetric database defines the seafloor for the model. This regional model spans 18ºS to 70ºN on a Mercator grid with a resolution of 1/12º latitude x 1/12º cos(y) longitude, where y is latitude. The initial temperature and salinity fields of the model are specified by the superposition of January 1990 monthly mean anomalies (Levitus et al., 1994a,b) and annual means (Boyer and Levitus, 1997). During the simulation, sea surface salinity was restored to the monthly climatology with a 15-day time scale. At the open boundaries of the model, temperature and salinity were maintained at climatological values. Flow through the southern boundary was specified by the Sverdrup relation while the northern boundary transport was based on output from a regional Arctic Ocean model (Brauch and Gerdes, 2005). The model was spun up from rest with 10 yrs of ECMWF (European Center for Medium-Range Weather Forecasting)

192 climatological forcing. The model was then forced with a superposition of the 1990–2004
193 monthly anomalies of the NCEP/NCAR (National Center for Environmental
194 Prediction/National Center for Atmospheric Research) reanalysis data (Kalnay et al.,
195 1996) and the climatological forcing applied during the spin up. Model temperature,
196 salinity, and velocity fields were stored as snapshots once every 3 days during the 1990–
197 2004 period.

198 Numerical trajectories of Lagrangian particles were calculated offline by integrating the
199 FLAME three-dimensional velocity field (Getzlaff et al., 2006; Hüttl-Kabus and Böning,
200 2008). More information about the trajectory calculation algorithm is documented in
201 Gary et al. (2011). Since vertical velocity information was not stored during the original
202 model run to conserve space, the vertical integral of the horizontal velocity divergence is
203 used to determine the vertical velocity at each time step.

204 FLAME output has been shown to compare favorably with observations in several
205 studies. Eden and Böning (2002) found good agreement in the width, maximum velocity
206 and transport of the mean boundary currents (West Greenland and Labrador Currents)
207 and with the spatial distribution, magnitude and seasonality of surface eddy kinetic
208 energy (EKE) in the Labrador Sea. Böning et al. (2006) showed that FLAME reproduced
209 the gradual increase in sea surface height in the Labrador Sea following the switch in the
210 sign of the North Atlantic Oscillation (NAO) index after 1994 that was observed with
211 altimetric sea surface height measurements (Hakkinen and Rhines, 2004), as well as the
212 decadal trends in the transport of the DWBC observed with current meters at 53ºN
213 (Dengler et al., 2006). Getzlaff et al. (2006) found good agreement between FLAME and
214 direct observations of the mean western boundary current transport at 53º and 43ºN, as

well as with subsurface EKE levels at 43ºN, where the model captured about 90% of the observed variability at 1500 m depth.

FLAME has been used to investigate particle dispersal in the subsurface North Atlantic in a number of studies (Bower et al., 2009; 2011; Burkholder and Lozier, 2011a; 2011b; 2014; Gary et al., 2011; 2012; 2014; Lozier et al., 2013; Kwon et al., 2014). Particularly relevant to the present study is a quantitative comparison between Lagrangian observations in the North Atlantic DWBC and simulated particle trajectories from FLAME by Lozier et al., (2013). These authors applied the Kolmogorov–Smirnov statistical test specifically designed for Lagrangian data by van Sebille et al. (2009) to compare (a) acoustically tracked subsurface float trajectories at 3000 dbar released in the DWBC between Newfoundland and Cape Hatteras in 1994 and 1995 (Bower and Hunt, 2000a, 2000b) to (b) similarly initiated numerical particle trajectories computed using FLAME. The time-varying test statistic, *Dn*, is the instantaneous maximum difference between cumulative probability distributions computed for the scatter of observed and simulated floats at each time step. If the trajectories in both ensembles are identical, *Dn*=0: the maximum value of *Dn* is 1. The power of the van Sebille et al. (2009) test is quantified by performing Monte Carlo iterations to determine the confidence level, alpha, around the test statistic. If alpha <0.05, we reject the null hypothesis that the trajectory ensembles come from the same spatial distribution. As documented in Lozier et al. (2013), visual comparison between the observed and simulated trajectories was favorable: the simulated pathways show evidence of offshore detrainment upstream of Cape Hatteras on a spatial scale comparable to the observed pathways. Also, the along-DWBC pathways simulated by the numerical particle trajectories were qualitatively

238 similar to the observed trajectories. The time average value of *Dn*=0.26 +/–0.05 with a
239 confidence level of alpha=0.92+/–0.08. Lozier et al. (2013) concluded therefore that the
240 spatial distributions of the observed and simulated trajectories were statistically
241 indistinguishable. This result is consistent with a similar comparison between observed
242 and simulated trajectories initiated in the DWBC near 50ºN at 700 and 1500 dbar (Gary
243 et al., 2011).

244 Figure 2a shows the time-mean model current speed perpendicular to the transect shown
245 in Figure 1a, which coincides with "Line W", a section that was occupied with a moored
246 array including current meters, T/S sensors and moored profilers from 2004-2014 (first
247 four years are described in Toole et al., 2011). The four simulated particle release sites
248 are shown by black dots with circle. The model DWBC is evident as negative mean flow
249 blanketing the continental slope between the 400-m and 4000-m isobaths. The strongest
250 mean DWBC flow exists at about 700 m, where it is more than 10 cm/s toward the
251 southwest. A second velocity extremum is at 3400 m over the 3800 m-isobath, where
252 mean current speed is about 4 cm/s. The strong northeastward mean model flow is
253 indicative of the Gulf Stream, located just offshore of the DWBC in this location (Figure
254 1a). For comparison, Figure 2b shows the 4-year mean along-slope current speed from
255 the Line W current observations. The shallow and deep DWBC velocity cores in Figure
256 2a are also apparent in the observations: centered at about 600 m over the mid-slope,
257 where peak southwestward speeds were about 8 cm/s, and above the 3700-m isobath,
258 where the mean DWBC speed was about twice as large as in the model at 8 cm/s. A third
259 slightly weaker velocity core not seen in the model was observed at about the 2750-m
260 isobath. As in the model section, the opposing Gulf Stream flow was observed by the

261 Line W array, although at a more offshore position. This data-model difference is not
262 surprising: EGCMs are notorious for not accurately reproducing the exact Gulf Stream
263 separation latitude. While this may impact the details of where exactly individual
264 particles first encounter the Gulf Stream, it is not expected to significantly affect the
265 general results for several reasons: (1) the release positions for the model particles are all
266 well within the DWBC as defined in both the model and observations; (2) the more
267 inshore position of the model Gulf Stream may in fact be more representative of the
268 position of the Gulf Stream relative to the benthic sampling sites, which are closer to
269 Cape Hatteras (Figure 1a) where the Gulf Stream is closer to the slope; and (3) Lozier et
270 al. (2013) showed good statistical agreement between simulated and observed trjaectories
271 at 3000 m in this region.

272 2.2 Particle release details

273 Particle trajectories were initialized at 4 depths across the continental slope (Fig. 1) in the
274 deepest model layer at each location, which has a thickness of 250 m. Model velocity in
275 this layer is representative of the flow above the frictional bottom boundary layer.
276 Particles were released every 15 days from January 1, 1990 until the end of 2004
277 generating 360 simulated trajectories at each site. Their positions were recorded every 3
278 days. Releases were continuous throughout the years to better capture inter-annual
279 variability in deep-water flows and because it more closely mimics the year-round
280 reproductive biology typical of deep-water protobranchs (Tyler et al., 1994; Sheltema and
281 Williams, 2009). Protobranch bivalves release pericalymma larvae that are thought to
282 disperse demersally for days to weeks (Zardus, 2002; Sheltema and Williams, 2009),
283 although the low temperatures at bathyal depths may extend development rates and PLDs

(O'Connor et al., 2007; Peck et al., 2007; Kelley and Eernisse, 2007). Recent estimates of PLDs for some deep-sea invertebrate larvae exceeded one year (Young et al., 2012). To estimate how larvae might disperse from sites on the continental slope near where bivalves have been sampled, we analyzed particle distributions and potential connectivity maps at 4 time scales; one month to approximate the PLD time inferred based on shallow-water relatives, 6 months and 1 year to consider potential dispersal if development times are extended due to the lower temperatures at bathyal depths and 5 years to quantify patterns based on multi-generational stepping-stone dispersal.

To provide a statistical description of particle trajectories (potential connectivity) we created contour maps that depict the frequency of particle visits to a particular model location (defined by a box with the same resolution as the model, 1/12º x 1/12º) over a specified time scale (i.e. 30, 180, 360, 1500 days). The position of each particle was recorded every 3 days and grid box counters were incremented by the number of particle visits in each box. This provides a contour plot of the particle positions (on 3 day intervals) integrated over the first 30 (180, 360 or 1500) days. Although this allows a single particle to increment a specific grid box more than once (either due to repeat visits resulting from convoluted trajectories or by slow advection where they remain in a single grid for more than three days) it represents a quantitative picture of the integrated potential connectivity. The probability that a larva settles within a particular spatial grid should be proportional to the particle visits. Since we do not know the exact PLDs of most deep-sea organisms or when they become competent to settle, it seems prudent to estimate connectivity using PLD "windows" (e.g. 0-30 days, 0-180 days, etc.).

307

308

309 **3. Results**

310 3.1 Trajectories

311 Individual particle trajectories indicated that neutrally buoyant particles did not typically
312 remain trapped in the mean southwest flow of the DWBC, but instead followed complex,
313 highly convoluted paths that often resulted in cross slope transport (Fig. 3). While initial
314 particle transport was often southwest, particles soon began to drift more eastward or
315 westward moving across slope, indicating dispersal across depth regimes was possible.
316 Off-shore transport appeared to be considerably more likely than on-shore, although both
317 occurred.

318

319 3.2 Potential Connectivity Maps

320 The trajectory contour maps (Fig. 4-7) depict the frequency of particle visits at a specific
321 model location providing an estimate of potential connectivity - where passive-dispersing
322 larvae could have settled during a particular dispersal time frame (e.g. during the first 30
323 days). Essentially, these figures represent average (integrated over 15 years – 1990-2004)
324 potential connectivity maps. Through time the contour maps show how the cloud of
325 particles spread and how connectivity might change with different PLDs. The figures
326 also include the position of particles (orange dots) at a specific time (30, 180, 360 or 1500
327 days).

328

329 After 30 days (Fig. 4), the connectivity maps and particles overlap among adjacent depths
330 indicating they are likely to exchange some larvae despite the clear influence of the
331 DWBC. The least overlap occurs between the two deepest stations, which were
332 separated by somewhat larger distances (99 km). However, at longer time scales (Fig. 5-
333 7) the density maps overlap considerably suggesting even the two deeper sites would be
334 well connected.
335
336 The influence of the DWBC was most intense at the shallowest release points (1500 and
337 2000 m) and during the first 30 days as shown by the shape of the connectivity maps and
338 the position of the particles (Fig. 4). However, even at these depths and short time
339 frames, some particles moved north and east from the release points, against the
340 prevailing flow due to mesoscale variability. As with the individual particle trajectories
341 (Fig. 3), these synoptic patterns indicate that initial dispersal is southwestward, but
342 through time is strongly influenced by cross-slope processes that result in a more
343 eastward spreading cloud (Fig. 5-7). For example, at 1500 m, particles drifted primarily
344 southwestward along slope with little cross-slope transport for the first 30 days (Fig. 4).
345 By 180 days (Fig 5), across-slope transport increased with many particles dispersing
346 eastward from the release point. By 1500 days (Fig. 7), transport includes many
347 trajectories that spread north and east, probably because they were entrained in the deep
348 flows of the Gulf Stream and were advected northeast (see also Bower and Hunt, 2000a,
349 2000b). Surprisingly, for particles released at 1500m, relatively few trajectories made it
350 south of 30° N.
351

352 In contrast, at 3200m, the initial spread of particles (first 30 days) is much more uniform
353 around the release point, probably because of the weaker bottom slope and/or weaker
354 mean flows compared to the variability at this depth (Fig. 4). By 180 or 360 days (Fig. 5-
355 6), dispersal appears largely similar to that at 1500m, but with a somewhat reduced
356 southwestward drift. Interestingly, by 1500 days, the deeper sites experience a much
357 greater southwestward drift, with many trajectories moving south of 30°N, probably
358 because the particles have slipped under the deeper flows of the Gulf Stream and were
359 advected southwest by the DWBC (Bower and Hunt, 2000a; 2000b). The trajectories at
360 3200m also include a considerable number that have moved eastward and some that have
361 moved westward onshore. Table 1 gives the percentage of particles at each release depth
362 that are offshore (in deeper water) of their release isobath after each of the time steps
363 examined. Particles are transported offshore more quickly at the shallower depths, and
364 after 30 days, the deepest site shows a slight onshore tendency. These results are
365 consistent with the idea that the Gulf Stream presents a more formidable barrier to
366 continuous southwestward transport along the slope in the DWBC for the shallower
367 particles (Bower and Hunt, 2000a, b).
368
369 In general, advection to the southwest appears to be a function of depth, with greater
370 southwest transport for the shallower sites during the first 360 days, especially the first 30
371 days (note the shape and dimensions of the red regions). By 1500 days, the pattern
372 reverses with greater southwest transport for the deeper release points and a surprising
373 northeastward spread for the shallowest site. At all depths, some trajectories moved
374 across slope through time.

3.3 Particle Displacement

If we consider only displacement from the release points, the distance traveled by particles varied with depth, but not in a simple predictable manner. The mean distance of particles from their release point after 30 days was greatest for the 2000 and 3200 m sites and least at 2500 m (Fig. 8). After 180 days, particles released at the two shallower depths (1500 and 2000 m) were displaced further than those at the deeper sites, and this was also true at 360 days. By 1500 days, displacements were similar for the 3 deepest release points and somewhat smaller for the shallowest depth.

The distribution of displacement distances typically had strong modes and were skewed right with a long tail of particles that dispersed much greater distances than the mean. After 30 days, the mean displacement was 27-58 km (depending on release depth), but some particles were more than 200 km from the release point. Similarly, after 1500 days, the mean displacement was ≈ 1100-1400 km, but some particles traveled nearly 5000 km from their release point.

4. Discussion

4.1 Dispersal Rates and Geography

Despite its importance to the ecology, evolution, and conservation of deep-sea organisms, little is known about how larvae might disperse at depth in the deep ocean and what implications that might have for the nature, scale and intensity of connectivity. Our

396 results are based on passively dispersing neutrally buoyant particles that provide a
397 qualitative picture of how the physics might move larvae, without any biology. Larvae
398 are unlikely to remain passive or neutrally buoyant during development, so the results
399 provide an important initial null model of how deep-water currents might affect dispersal.

400 The numerical simulations indicated that larvae would disperse on average about 1-2 km
401 d^{-1} at mid to lower bathyal depths in the western North Atlantic. This is considerably less
402 than dispersal estimates based on numerical simulations of coastal circulation in shallow
403 water (< 200 m) (Siegel et al., 2008, Mitari et al., 2009, Watson et al., 2010, Drake et al.,
404 2011, Kim and Barth, 2011) and often less than what has been found at shallower bathyal
405 depths (Yearsley and Sigwart, 2011; Young et al., 2012; Sala et al., 2013). For example,
406 simulated passive dispersal based on models of coastal circulation varied from 3-7 km d^{-}
407 ^{1}, depending on depth (1-75 m), along the Oregon coast (Kim and Barth, 2011) and 2-8
408 km d^{-1} for depths < 20 m along the California coast (Drake et al., 2011). Even at deeper
409 upper bathyal depths median dispersal rates were 1-6 km d^{-1}, depending on depth (100 or
410 500 m) and taxon, in the Northwest Atlantic and Gulf of Mexico (Young et al., 2012),
411 while dispersal rates were 1- 4 km d^{-1} at 800-1440 m in the tropical South Pacific
412 (Yearsley and Sigwart, 2011) and only about 0.5 km d^{-1} at 600-2000m in the Northeast
413 Atlantic (Sala et al., 2013). At abyssal depths, dispersal rates are likely to be significantly
414 less because the currents are substantially slower (Hogg and Owen 1999). Dispersal rates
415 in general appear to decline with depth, however, the distances larvae disperse and the
416 degree of connectivity will also depend on PLDs, which are likely to be longer in the
417 deep sea due to slower developmental rates at lower temperatures (O'Connor et al.,
418 2007). The PLDs of some deep-water taxa are greater than a year and can exceed 600

419 days (Arellano and Young, 2009; Bennett et al., 2012; Young et al., 2012).

420 Although the mean distance our simulated particles dispersed was relatively small, the
421 dispersal kernel was skewed strongly to the right with some particles dispersing much
422 greater distances – up to 4-times the mean (Fig. 8). Rare long distance transport of larvae
423 may have little impact demographically, but play an important role on longer time scales
424 because it can maintain evolutionary-connectivity among distant populations, affect the
425 spatial and temporal scales of divergence, foster range shifts or expansions, enhance
426 metapopulation and metacommunity persistence, and provide a mechanism to escape
427 localized disturbances (Trakhtenbrot et al., 2005; Nathan, 2006; Hellberg, 2009).

428 4.2 Genetic Patterns, Connectivity and the Influence of the DWBC

429 Both the individual particle trajectories and their distributions indicate that the DWBC is
430 unlikely to impede larval exchange between upper and lower bathyal depths in this region
431 of the Northwest Atlantic. This is consistent with empirical estimates of dispersal from
432 floats released within the DWBC (Bower and Hunt, 2000a; 2000b; Bower et al., 2009;
433 Bower et al., 2011; 2013) and with simulated trajectories (based on FLAME) from
434 thousands of e-floats released into the DWBC at various locations within the North
435 Atlantic (Bower et al., 2009; Gary et al., 2011; Lozier et al. 2013). Most trajectories were
436 highly convoluted and departed significantly from the mean southwestward flow of the
437 DWBC. Movement across depths (east or west) was common indicating that the DWBC
438 is unlikely to prevent the exchange among depths of passively dispersing larvae,
439 assuming larvae survive the environmental changes (e.g. temperature, pressure, etc.) that
440 attend changes in depth.

441 The cross-slope dispersal of particles documented here and in earlier work is not
442 necessarily representative of the entire continental slope of the western North Atlantic,
443 but nor is it unique. The primary cause of the large cross-slope excursions in the vicinity
444 of the bottom sampling sites is interaction between the DWBC and Gulf Stream. At about
445 35N, the present-day Gulf Stream curves from its northward path toward the northeast
446 and crosses the continental slope and proceeds generally eastward over deep water. This
447 separation latitude is not fixed but wanders north and south due to meandering of the
448 Gulf Stream. Particles being carried southwestward by the DWBC over the mid- and
449 upper-slope north of the separation point are almost always entrained into the Gulf
450 Stream as the two currents converge near the separation latitude. This results in particles
451 being swept offshore into deeper water (see Bower and Hunt, 2000a; 2000b).

452 On the other hand, particles being advected by the deeper part of the DWBC are
453 frequently able to pass under the Gulf Stream and continue equatorward, but this too is
454 accompanied by cross-slope motion: conservation of potential vorticity (approximated
455 accurately at these depths by f/H, where f is the Corilis parameter and H is the water layer
456 thickness) dictates that the deep part of the water column slide down the slope by
457 hundreds of meters in order to slip beneath the deep thermocline of the subtropical gyre
458 (Hogg and Stommel, 1985; Bower and Hunt, 2000a; 2000b). These particles may then
459 continue equatorward over the slope but following a deeper isobath. This might also help
460 to explain the genetic similarity between North and South Atlantic populations of the
461 protobranch bivalve *Nucula atacellana* at lower bathyal depths (Zardus, 2006).

462 Disruption of along-slope flow of the DWBC by another current has also been well-
463 documented with observations around the Grand Banks of Newfoundland and Flemish

464 Cap, where the Gulf Stream and its northward extension, the North Atlantic Current
465 sometimes cross the continental slope and interact with the DWBC transport (Lavender et
466 al., 2000; Fischer and Schott, 2002; Rhein et al., 2002; Bower et al., 2009; 2011). Sharp
467 corners in the continental slope have also been shown to cause cross-slope motion of float
468 trajectories in the DWBC and even detrainment of the particles from the DWBC entirely
469 (Leaman and Vertes, 1996; Bower et al., 2013), likely due to inertial overshoot of the
470 sharp corner (see Bower et al., 1997 and references therein). In between regions of
471 current interactions and sharp bathymetric features, the DWBC in the western North
472 Atlantic generally flows mostly uninterrupted for hundreds of kilometers over the
473 continental slope, impeded from crossing the slope by potential vorticity (see examples
474 in Leaman and Vertes, 1996; Bower and Hunt, 2000a). These are regions where the
475 DWBC is most likely to impede larval exchange among depths. The locations of
476 enhanced cross-slope motions may have been different in the distant past when the Gulf
477 Stream may have separated at more southerly latitudes (e.g., Keffer et al., 1988) with
478 implications for how deep-water flows might influence connectivity over geological time.

479 Given the results from both modeled and empirical float estimates of dispersal, it seems
480 unlikely that the strong genetic divergence we find among bivalve populations above and
481 below 3000m in the western North Atlantic (Chase et al., 1998; Etter et al., 2005; Zardus
482 et al., 2006; Jennings et al., 2013; Glazier and Etter, 2014) reflects the restriction of gene
483 flow by the DWBC. If populations at different depths are well connected and dispersal
484 among depths is ongoing, how can such divergence emerge? The lack of obvious
485 physical transport mechanisms that would impede larval exchange and the small scale
486 over which divergence has occurred suggest selection may be involved.

Recent theoretical and empirical evidence clearly demonstrate that despite ongoing gene flow a variety of mechanisms can lead to diversification (reviewed in Nosil, 2012) and that these processes might be considerably more important for population differentiation and species formation in marine environments where physical barriers to gene exchange are less common (Bowen et al., 2013). For example, adaptation to local environmental conditions with ongoing gene flow (Doebeli and Dieckmann, 2003; Irwin, 2012) can lead to immigrant inviability (Nosil et al., 2005; Marshall et al., 2010), which will reduce gene flow and promote divergence. It is possible that larvae disperse among depths, but lack the necessary local adaptations to survive or reproduce.

Emerging phylogeographic patterns in the deep sea suggest that environmental gradients paralleling changes in depth may provide one of the primary mechanisms mediating population differentiation and species formation in deep-water ecosystems (Etter et al., 2005; Baco and Cairns, 2012; Jennings et al., 2013; Quattrini et al., 2013). Depth differences are associated with changes in a wide variety of environmental variables including temperature, hydrostatic pressure, oxygen, POC flux, habitat heterogeneity, trophic complexity and the nature and amount of food (reviewed in Gage and Tyler, 1991). These environmental changes have been invoked as key forces in regulating bathymetric distributions (Carney, 2005), altering ecological processes (Levin et al., 2001), shaping major macroecological patterns (reviewed in Rex & Etter, 2010), fostering adaptation (e.g. Somero, 1992; Levin, 2003; Brown & Thatje, 2014), and promoting diversification (Etter et al., 2005; Jennings et al., 2013). Widespread and consistent divergence across depth gradients suggests depth and its concomitant environmental gradients may also play an important role in the origin and evolution of

510 the deep-sea fauna.

511 4.3 Paleo-oceanography

512 Our estimates of dispersal and connectivity are based on the contemporary
513 hydrodynamics of the North Atlantic. The probability that larval exchange occurs among
514 depths is a function of the intensity of the DWBC and the strength of cross slope
515 processes. The oceanography of the North Atlantic and in particular the intensity of the
516 DWBC (Boyle and Keigwin, 1982; Keigwin and Pickart, 1999; McManus et al., 2004;
517 Lippold et al., 2012) and the position and strength of the Gulf Stream (Keffer et al.,
518 1988) have varied through time. It is possible that a more intense DWBC in the past
519 disrupted gene flow between depth regimes long enough for populations to diverge in
520 regions where cross-slope processes are weak (e.g. away from sharp bathymetric features
521 or interactions with the Gulf Stream). If divergence in the past was sufficient to prevent
522 recruitment of larvae from contrasting depth regimes, then even though the contemporary
523 flows of the DWBC allow larval exchange between depths now, gene flow might be
524 precluded due to migrant inviability (sensu Nosil et al., 2005). Molecular clock estimates
525 of the observed genetic divergence between upper and lower bathyal populations in the
526 protobranch *Nucula atacellana* suggest a recent split 1 mya (Jennings et al., 2013), during
527 which time the DWBC varied considerably in intensity (Boyle and Keigwin 1982;
528 Keigwin and Pickart, 1999; McManus et al., 2004; Lippold et al., 2012). The
529 protobranch *Neilonella salicensis* also exhibits a strong genetic break between depths in
530 the same general vicinity, but molecular clock estimates of divergence between shallow
531 and deep clades indicate gene flow has been absent for more than 15 million years
532 (Glazier and Etter, 2014). Interestingly, the formation of the North Atlantic Deep Water,

533 which drives the DWBC, has progressively weakened over the past 3 million years and
534 was considerably stronger 3 to 14 mya (Frank et al. 2002). Our estimates of divergence
535 time in these bivalves coincide with this period of stronger export. As global climate
536 shifted historically and thermohaline circulation waxed and waned the DWBC may have
537 periodically disrupted gene flow among populations at different depths fostering repeated
538 rounds of species formation. If true, we should expect other taxa with distributions that
539 span the DWBC to exhibit diversification at similar times. In addition, the waxing and
540 waning of the DWBC might act essentially as a speciation pump by repeatedly disrupting
541 gene flow in regions of weak cross-slope forces, which might help explain the well
542 known peak in diversity at bathyal depths in the western North Atlantic.

543 4.4 Caveats

544 Although the estimates of dispersal presented here represent a reasonable first
545 approximation of how larvae might disperse at depth, a number of factors have not been
546 included that are likely to alter dispersal and the scale and intensity of connectivity. They
547 were excluded for simplicity and because we lack reasonable estimates of those factors.
548 For example, larval behavior such as tidal, diurnal or ontogenetic migration can
549 dramatically alter the scale and direction larvae disperse (Drake et al. 2013; Morgan
550 2014). This often depends on stratified water columns where vertical migration over
551 relatively small scales allows larvae to modulate dispersal by exploiting water masses
552 moving at different rates or directions. In the deep sea, stratification is less,
553 environmental cues are less pronounced (e.g. diurnal, tidal) and larvae would in general
554 need to migrate over much greater distances to find water masses that differ significantly
555 in speed or direction (e.g. DWBC vs Gulf Stream, Fig. 2). We know little about the

556 behavior of deep-sea larvae, but recent evidence identified bathyal mussel larvae
557 (*Bathymodiolus*) in the surface waters (Arellano et al. 2014), suggesting such vertical
558 migrations are possible. Larvae of other deep-sea taxa have also been found in surface
559 waters (Reviewed in Scheltema, 1994; Bouchet and Waren, 1994; Young, 2003). The
560 scale and geography of dispersal for larvae in the surface currents would be substantially
561 different than those dispersing at depth. While dispersing in the surface currents might be
562 possible for some deep-sea taxa, many species are confined to deep water because their
563 larvae cannot tolerate the low pressure and high temperature of near-surface waters
564 (Young and Tyler, 1993; Young et al., 1996; 1998; Brooke and Young, 2009; Bennett et
565 al., 2012). Demersal larvae might also exploit the slower flows of the benthic boundary
566 layer to limit dispersal away from natal sites.

567 Another important factor not included in our simulation is how and when larvae descend
568 through the water column to settle, which might involve considerable changes in depth
569 and water masses for larvae that migrate ontogenetically to surface waters or for those
570 advected from the slope into deeper waters. Settlement might be active (e.g. swimming)
571 or passive (e.g. density changes) (reviewed in Young, 2003), and could alter dispersal
572 and how populations are connected. Better estimates of dispersal and connectivity in the
573 deep sea will require more details about larval behavior and development at depth. In
574 addition, spatial variation in fecundity, mortality during the larval phase and larval
575 physiological tolerance needs to be included because they can influence dispersal and
576 population connectivity (Treml et al., 2012; White et al., 2014).

577 Our estimates of dispersal and connectivity are also dependent on the quality of the
578 hydrographic model driving dispersal. It is important to keep in mind that the resolution

579 of the physical transport model might be inadequate to capture all the forces affecting
580 dispersal on the scale of minute larvae. Biophysical models can be enormously insightful
581 in understanding how transport processes might influence dispersal (e.g. Xue et al., 2008;
582 Siegel et al., 2008; Inzce et al., 2010; Watson et al., 2010; Drake et al., 2011) and to
583 explore how larval behaviors and life histories might affect connectivity (Drake et al.,
584 2013; Morgan, 2014; Treml et al., 2012; White et al., 2014). However, before using them
585 directly to estimate potential impacts of contemporary environmental issues (e.g. resource
586 exploitation, mining, etc.) or to guide conservation strategies (e.g. MPA design), they
587 need to be empirically validated on both ecological and evolutionary time scales
588 (reviewed in Levin, 2006; Kool et al., 2013). Trace element signatures using calcified
589 structures (e.g. López-Duarte et al., 2012) or genetic analyses of early recruits (e.g. Jones
590 et al. 2005) could be used to estimate connectivity on ecological (demographic) time
591 scales. On longer evolutionary time scales, estimates of population genetic divergence
592 (e.g. Galindo et al., 2006; 2010; Weersing and Toonen, 2009; White et al., 2010; Alberto
593 et al., 2011) can provide insight into average long-term connectivity.

594 4.5 Conclusions

595 The results presented here provide one of the first estimates of how passive larvae might
596 disperse at deeper bathyal depths in the western North Atlantic and quantifies the scale
597 and geography of how populations might be connected. Unraveling how populations are
598 connected is critical for explaining biogeographic patterns of diversity (Levin and Dayton
599 2009; Gooday et al., 2010), predicting how deep-sea ecosystems might respond to
600 climate change (Danovaro et al., 2008; 2009; Glover et al., 2010), developing
601 conservation and management strategies to mitigate the intense exploitation of deep-sea

resources (Ramírez-Llodra et al., 2011; Levin and Sibuet, 2012; Mengerink et al., 2014; Pusceddu et al., 2014) and identifying appropriate locations and scales for MPAs (Harris and Whiteway, 2009; Clark et al., 2011; Watling et al., 2013).

Acknowledgments

The authors are deeply grateful to S. Gary of the Scottish Association of Marine Science for providing the numerical particle trajectories used in this analysis and for his assistance in a preliminary version of figure 2. We also thank H. Furey of WHOI for her expert assistance with data representation ideas and figure preparation, and the captain and crew of the R/V *Endeavor* and all participants of cruise EN447 for help in collecting and sorting samples used for genetic estimates of population connectivity. RJE owes a special debt of gratitude to Howard Sanders for providing the bivalves many years ago from his extensive collection that allowed us to begin to explore evolutionary questions in the deep Atlantic. This work benefitted from thoughtful discussions and comments from John Toole, Lloyd Keigwin, and Paige Logan, and insightful comments from three anonymous reviewers. ASB was supported by Grant No. OCE-0926656 to WHOI by the U.S. National Science Foundation and RJE was supported by NSF Grants OCE0726382 and OCE1130541.

622 **References**
623
624 Adams, D.K., Mullineaux, L.S., 2008. Supply of gastropod larvae to hydrothermal vents
625 reflects transport from local larval sources. Limnol. Oceanogr. *53*, 1945.

626 Alberto, F., Raimondi, P.T., Reed, D.C., Watson, J.R., Siegel, D.A., Mitarai, S., Serrao,
627 E. A., 2011. Isolation by oceanographic distance explains genetic structure for
628 *Macrocystis pyrifera* in the Santa Barbara Channel. Mol. Ecol. 20, 2543-2554.

629 Arellano, S.M., Young, C.M., 2009. Spawning, development, and the duration of larval
630 life in a deep-sea cold-seep mussel. Biol. Bull. *216*, 149-162.

631 Arellano, S. M., Van Gaest, A. L., Johnson, S. B., Vrijenhoek, R. C., & Young, C. M.
632 2014. Larvae from deep-sea methane seeps disperse in surface waters. Proc. R. Soc. B
633 *281*, 20133276.

634 Baco AR, Cairns SD. 2012. Comparing molecular variation to morphological species
635 designations in the deep-sea coral *Narella* reveals new insights into seamount coral
636 ranges. PLOS ONE, 7: e45555. PubMed: 23029093.

637 Baco, AR, RJ Etter, P Beerli, B Kinlan, P Ribeiro, S von der Heyden, and A. Thaler.
638 2015. A synthesis of dispersal distances in deep-sea fauna inferred from genetic data:
639 implications for connectivity and MPA design.

640 Baums, I. B., Paris, C. B., & Chérubin, L. M. 2006. A bio-oceanographic filter to larval
641 dispersal in a reef-building coral. Limnol. Oceanogr. *51*, 1969-1981.

642 Beckmann, A., Döscher, R., 1997. A method for improved representation of dense water
643 spreading over topography in geopotential-coordinate models. J. Phys. Oceanogr. 27,
644 581–591.

645 Bennett KC, Young CM, Emlet RB., 2012. Larval development and metamorphosis of
646 the deep-sea cidaroid urchin Cidaris blakei. Biol Bull 222:105–17.

647 Biastoch,A., Böning,C.W.,Getzlaff,J.,Molines,J.M.,Madec,G., 2008. Causes of
648 interannual–decadal variability in the meridional overturning circulation of the
649 midlatitude North Atlantic Ocean. J. Climate 21, 6599–6615.

650 Böning, C.W., Scheinert, M., Dengg, J., Biastoch, A., Funk, A., 2006. Decadal variability
651 of subpolar gyre transport and its reverberation in the North Atlantic overturning.
652 Geophys. Res. Lett. 33, L21S01 http://dx.doi.org/10. 1029/2006GL026906.

653 Botsford, L., D. Brumbaugh, C. Grimes, J. Kellner, J. Largier, M.O. Farrell, S. Ralston,
654 E. Soulanille, and V. Wespestad. 2009. Connectivity, sustainability, and yield:
655 bridging the gap between conventional fisheries management and marine protected
656 areas. Rev. Fish. Biol. Fisheries 19:69-95.

657 Botsford, L., Micheli, F. and Hastings, A. 2003. Principles for the design of marine

reserves. Ecol. Appl. 13:25-31.

Bowen B.W., Rocha L.A., Toonen R.J., Karl S.A., Laboratory T.T., 2013. The origins of tropical marine biodiversity. Trends Ecol. Evol. 28: 359–366.

Bower, A, S., R. M. Hendry, D. E. Amrhein, and J.M. Lilly. 2013. Direct observations of formation and propagation of subpolar eddies into the Subtropical North Atlantic. Deep-Sea Res. Part II, *85*, 15-41.

Bower, A. S., Lozier, M. S., Gary, S.F., Böning, C.W. 2009. Interior pathways of the North Atlantic meridional overturning circulation. Nature, *459*, 243-247.

Bower, A. S., S. Lozier, and S. Gary, 2011. Export of Labrador Sea Water from the subpolar North Atlantic: A Lagrangian perspective. Deep-Sea Res. Part II 58:1798-1818.

Bower, A., Hunt, H.D., 2000a. Lagrangian observations of the deep western boundary current in the North Atlantic Ocean. Part I: large-scale pathways and spreading rates. J. Phys. Oceanogr. 30, 764–783.

Bower, A., Hunt, H.D., 2000b. Lagrangian observations of the deep western boundary current in the North Atlantic Ocean. Part II:the Gulf Stream-deep western boundary current crossover. J. Phys. Oceanogr. 30, 784–804.

Boyer, T.P., Levitus, S. 1997. Objective Analyses of temperature and salinity for the world ocean on a 1/4 grid. NOAA/NESDIS Atlas 11. Washington D.C.: U.S. Gov. Printing Office.

Boyle EA, Keigwin LD. 1982. Deep circulation of the North Atlantic over the last 200,000 years: geochemical evidence. Science 218: 784–787.

Bradbury, I. R., Laurel, B., Snelgrove, P. V., Bentzen, P., Campana, S. E. 2008. Global patterns in marine dispersal estimates: the influence of geography, taxonomic category and life history. Proc. R. Soc. B. *275*, 1803-1809.

Brauch, J.P., Gerdes, R., 2005. Response of the northern North Atlantic and Arctic oceans to a sudden change of the North Atlantic oscillation. J. Geophys. Res. 110, C11018 http://dx.doi.org/10.1029/2004JC002436.

Brooke S.D., Young C.M. 2009. Where do the embryos of *Riftia pachyptila* develop? Pressure tolerances, temperature tolerances, and buoyancy during prolonged embryonic dispersal. Deep-Sea Res II 56:1599–1606

Brown, S. E., Thatje, S. 2014. Explaining bathymetric diversity patterns in marine benthic invertebrates and demersal fishes: physiological contributions to adaptation of life at depth. Biol Rev. *89*, 406-426.

Burkholder and M.S. Lozier, 2014. Tracing pathways of the North Atlantic meridional

693 overturning circulation's upper limb. Geophysical Research Letters, 41, 4254-4260.

694 Burkholder, K.C. and M. S. Lozier, 2011. Mid-depth Lagrangian pathways in the eastern
695 North Atlantic and their impact on the salinity of the eastern subpolar gyre. Deep-Sea
696 Res. I, 58, 1196-1204.

697 Burkholder, K.C. and M. S. Lozier, 2011. Subtropical to subpolar pathways in the North
698 Atlantic. J. Geophys. Res. – Oceans, 116, C07017, doi:10.1029/2010JC006697.

699 Byers, J. E., Pringle. J. M. 2006. Going against the flow: retention, range limits and
700 invasions in advective environments. Mar. Ecol. Prog. Ser. 313:27–41.

701 Carney RS. 2005. Zonation of deep biota on continental margins. Oceanogr. Mar. Biol.
702 Ann. Rev. 43, 211–278.

703 Caswell, H., Neubert, M. G., Hunter, C. M. 2011. Demography and dispersal: invasion
704 speeds and sensitivity analysis in periodic and stochastic environments. Theor. Ecol.
705 *4*, 407-421.

706 Chase MR, Etter RJ, Rex MA, Quattro JM. 1998. Bathymetric patterns of genetic
707 variation in a deep-sea protobranch bivalve, *Deminucula atacellana*. Mar. Biol. 131,
708 301–308.

709 Clark MR, Watling L, Rowden AA, Guinotte JM, 2011. A global seamount classification
710 to aid the scientific design of marine protected area networks. Ocean Coastal Manag.
711 54, 19–36.

712 Cowen, R.K., Sponaugle, S. 2009. Larval dispersal and marine population connectivity.
713 Ann. Rev. Mar. Sci. 1:443-466.

714 Danovaro, R., Corinaldesi, C., Luna, G. M., Magagnini, M., Manini, E., Pusceddu, A.
715 2009. Prokaryote diversity and viral production in deep-sea sediments and seamounts.
716 Deep-Sea Res. II. *56*, 738-747.

717 Danovaro, R., Gambi, C., Dell'Anno, A., Corinaldesi, C., Fraschetti, S., Vanreusel, A.,
718 Vincx, M. Gooday, A. J. 2008. Exponential decline of deep-sea ecosystem
719 functioning linked to benthic biodiversity loss. Curr. Biol., *18*, 1-8.

720 Dengler, M., Fischer, J., Schott, F.A., Zantopp, R., 2006. Deep Labrador Current □and
721 its variability in 1996–2005. Geophys. Res. Lett. 33. doi:10.1029/
722 □2006GL026702.□

723 Doebeli M, Dieckmann U, 2003. Speciation along environmental gradients. Nature 421,
724 259–264. doi:10.1038/nature01274. PubMed: 12529641.

725 Drake, P. T., Edwards, C. A., Barth, J. A. 2011. Dispersion and connectivity estimates
726 along the US west coast from a realistic numerical model. J. Mar. Res. *69*, 1-37.

727 Drake, P. T., Edwards, C. A., Morgan, S. G., & Dever, E. P. 2013. Influence of larval
728 behavior on transport and population connectivity in a realistic simulation of the
729 California Current System. J. Mar. Res. *71*, 317-350.

730 Eden, C., Boening, C., 2002. Sources of eddy kinetic energy in the Labrador Sea. J.
731 Phys. Oceanogr. 32, 3346–3363. doi:10.1175/15200485(2002)032(3346:
732 SOEKEI)2.0.CO;2.

733 Etter RJ, Grassle F. 1992. Patterns of species diversity in the deep sea as a function of
734 sediment particle size diversity. Nature 360: 576–578.

735 Etter, R.J., Rex, M.A. Chase, M., Quattro. J. 2005. Population differentiation decreases
736 with depth in deep-sea bivalves. Evolution 59, 1479-1491.

737 Fischer, J., Schott, F.A., Dengler, M., 2004. Boundary circulation at the exit of the
738 Labrador Sea. J. Phys. Oceanogr. 34, 1548–1570.

739 Frank, M., Whiteley, N., Kasten, S., Hein, J. R., and O'Nions, K. 2000. North Atlantic
740 Deep Water export to the Southern Ocean over the past 14 Myr: Evidence from Nd
741 and Pb isotopes in ferromanganese crusts. Paleoceanography, *17*, 1-9.

742 Gage JD, Tyler PA. 1991. *Deep-sea biology: a natural history of organisms at the deep-*
743 *sea floor*. Cambridge, UK: Cambridge University Press.

744 Gaines, S. D., White, C. Carr, M.H., Palumbi, S.R. 2010. Designing marine reserve
745 networks for both conservation and fisheries management. Proc. Natl. Acad. Sci.
746 USA 10, 18286-18293.

747 Gaines, S.D., Gaylord, B. Largier, J. 2003. Avoiding current oversights in marine
748 reserve design. Ecol. Appl. 13, 32-46.

749 Galindo H., Olson D., Palumbi S., 2006. Seascape genetics: A coupled oceanographic-
750 genetic model predicts population structure of Caribbean corals. Curr. Biol., 16,
751 1622–1626.

752 Galindo, H.M., Pfeiffer-Herbert, A.S., McManus, M.A., Chao, Y., Palumbi. S.R. 2010.
753 Seascape genetics along a steep cline: Using genetic patterns to test predictions of
754 marine larval dispersal. Mol. Ecol. 19, 3692-3707.

755 Gary, S.F., M.S. Lozier, A. Biastoch, C.W. Böning, 2012. Reconciling tracer and float
756 observations of the export pathways of Labrador Sea Water, Geophys. Res. Lett. 39,
757 L24606, doi:10.1029/2012GL053978.

758 Gary, S.F., M.S. Lozier, Y.O. Kwon, and J.J. Park, 2014. The fate of North Atlantic
759 subtropical mode water in the FLAME model. J. Phys. Oceanogr. 44, 1354-1371.

760 Gary,S.F.,Lozier,M.S., Böning,C.,Biastoch,A., 2011. Deciphering the pathways for the
761 deep limb of the meridional overturning circulation. Deep-Sea Res. 58, 1781–1797.

762 Getzlaff, K., Boening, C.W., Dengg, J., 2006. Lagrangian perspectives of deep water
763 export from the subpolar North Atlantic. Geophys. Res. Lett. 33. doi:10.1029/
764 2006GL026470.

765 Getzlaff, K.C., Böning, C.W., Dengg, J., 2006. Lagrangian perspectives of deep water
766 export from the subpolar North Atlantic. Geophys. Res. Lett. 33, L21S08 http://
767 dx.doi.org/10.1029/2006GL026470.

768 Glazier, AE, Etter. RJ 2014. Cryptic speciation along a bathymetric gradient Biol. J. Lin.
769 Soc. 113, 897-913.

770 Glover, A. G., Gooday, A. J., Bailey, D. M., Billett, D. S. M., Chevaldonné, P., Colaco,
771 A., Copley J., Cuvelier D., Desbruyeres D., Kalogeropoulou V., Klages M.,
772 Lampadariou N., Lejeusne C., Mestre N., Paterson G. L. J., Perez T., Ruhl H.,
773 Sarrazin J., Soltwedel T., Soto E. H., Thatje S., Tselepides A., Van Gaever S.,
774 Vanreusel, A. (2010). Temporal change in deep-sea benthic ecosystems: a review of
775 the evidence from recent time-series studies. Adv. Mar. Biol. *58*, 1-95.

776 Gooday, A. J., Bett, B. J., Escobar, E., Ingole, B., Levin, L. A., Neira, C., Raman, A.V.,
777 Sellanes, J. 2010. Habitat heterogeneity and its influence on benthic biodiversity in
778 oxygen minimum zones. Mar. Ecol., *31*, 125-147.

779 Hakkinen, S., Rhines, P.B., 2004. Decline of subpolar North Atlantic circulation during
780 the 1990s. Science 304, 555–559. doi:10.1126/science.1094917.

781 Hanski, I. 1999. *Metapopulation ecology*. Oxford University Press, New York, New
782 York, USA.

783 Harris PT, Whiteway T. 2009 High seas marine protected areas: Benthic environmental
784 conservation priorities from a GIS analysis of global ocean biophysical data. Ocean
785 Coastal Manag. 52: 22– 38.

786 Hellberg ME 2009. Gene flow and isolation among populations of marine animals. Annu
787 Rev. Ecol. Evol. Syst. 40, 291–310. doi:10.1146/ annurev.ecolsys.110308.120223.

788 Henry, L. A., Frank, N., Hebbeln, D., Wienberg, C., Robinson, L., de Flierdt, T. V., ... &
789 Roberts, J. M. 2014. Global ocean conveyor lowers extinction risk in the deep sea.
790 Deep-Sea Res I. *88*, 8-16.

791 Hogg N.G., Stommel, H. 1985. On the relation between the deep circulation and the Gulf
792 Stream. Deep-Sea Res. I. 32, 1181–1193.

793 Hogg N.G., Owens W.B. 1999 Direct measurement of the deep circulation within the
794 Brazil Basin. Deep-Sea Res. II, 46, 335–353.

795 Holt, R.D. 1985 Population dynamics in two-patch environments: Some anomalous
796 consequences of an optimal habitat distribution. Theor. Pop. Biol. ***28***, 181–208.

797 Hubbell, S.P. 2001. The Unified Neutral Theory of Biodiversity and Biogeography.

798 Princeton University Press, Princeton, NJ.

799 Hüttl-Kabus ,S., Böning, C.W.,2008. Pathways and variability of the off-equatorial
800 undercurrents in the Atlantic Ocean. J. Geophys. Res. 113, C10018 http://dx.
801 doi.org/10.1029/2007JC004700.

802 Inzce, L., Xue, H., Wolff, N., Xu, D., Wilson, C., Steneck, R., Wahle, R., Lawton, P.,
803 Pettigrew, N., Chen, Y. 2010. Connectivity of lobster (*Homarus americanus*)
804 populations in the coastal Gulf of Maine: part II. Coupled biophysical dynamics. Fish.
805 Oceanogr. 19:1-20.

806 Irwin DE 2012 Local adaptation along smooth ecological gradients causes
807 phylogeographic breaks and phenotypic clustering. Am. Nat. 180: 35–49.
808 doi:10.1086/666002. PubMed: 22673649.

809 Jennings R.M., Etter, R.J. and Ficarra. L. 2013. Population differentiation and species
810 formation in the deep sea: the potential role of environmental gradients and depth.
811 *PLoS ONE* 8(10): e77594.

812 Jones, G. P., Planes, S., Thorrold, S. R. 2005. Coral reef fish larvae settle close to home.
813 *Curr. Biol.*, *15*, 1314-1318.

814 Kalnay, E., Kanamitsu, M., Kistler, R., Collins, W., Deaven, D., Gandin, L., Iredell, M.,
815 Saha, S., White, G., Woollen, J. Zhu, Y. Leetmaa, A. Reynolds, R., Chelliah, M.
816 Ebisuzaki, W., Higgins, W., Janowiak, J., Mo, K.C., Ropelewski, C., Wang, J., Jenne, R.
817 Joseph, D. 1996. The NCEP/NCAR 40-year reanalysis project. Bull. Amer. Meteorol.
818 Soc. *77*, 437-471.

819 Keffer, T., D.G. Martinson, B.H. Corliss, 1988. The position of the Gulf Stream during
820 quaternary glaciations. Science, 241, 440-442.

821 Keigwin LD, Pickart RS. 1999. Slope water current over the Laurentian Fan on
822 interannual to millennial timescales. Science 286, 520–523.

823 Kelly, R. P., Eernisse, D. J. 2007. Southern hospitality: a latitudinal gradient in gene
824 flow in the marine environment. Evolution, *61*, 700-707.

825 Kim, S., Barth, J. A. 2011. Connectivity and larval dispersal along the Oregon coast
826 estimated by numerical simulations. J. Geophy.Res.- Oceans *(1978–2012)*, *116*(C6).
827 doi/10.1029/2010JC006741

828 Kinlan, B.P., Gaines, S.D. 2003. Propagule dispersal in marine and terrestrial
829 environments: a community perspective. Ecology 84, 2007-2020.

830 Kool, J. T., Moilanen, A., Treml, E. A. 2013. Population connectivity: recent advances
831 and new perspectives. Landsc. Ecol. *28*, 165-185.

832 Kwon, Y. O., Park, J. J., Gary, S. F., Lozier, M. S. 2015. Year-to-year re-outcropping of

833 Eighteen Degree Water in an eddy-resolving ocean simulation. J. Phys. Oceanogr. in
834 press.

835 Lavender, K.L., Davis, R.E., Owens, W.B., 2000. Mid-depth recirculation observed in the
836 interior Labrador and Irminger seas by direct velocity measurements. Nature 407, 66–
837 69.

838 Leaman, K. D., Vertes, P. S., 1996: Topographic influences on recirculation in the deep
839 western boundary current: Results from RAFOS float trajectories between the Blake–
840 Bahama Outer Ridge and the San Salvador ''Gate.'' J. Phys. Oceanogr., **26,** 941–961.

841 Leibold, M.A., M. Holyoak, N. Mouquet, P. Amarasekare, J.M. Chase, M.F. Hoopes,
842 R.D. Holt, J.B. Shurin, R. Law, D. Tilman, M. Loreau, and A. Gonzalez. 2004. The
843 metacommunity concept: A framework for multi-scale community ecology. Ecol.
844 Lett. 7, 601-613.

845 Leis, J., Van Herwerden, L., Patterson. H.M. 2011. Estimating connectivity in marine
846 fish populations: what works best? Oceanogr. Mar. Biol. Ann. Rev. 49:193-234.

847 Levin LA, Sibuet M. 2012. Understanding continental margin biodiversity: a new
848 imperative. Ann. Rev. Mar. Sci. 4, 79–112.

849 Levin, L. A., Dayton, P. K. 2009. Ecological theory and continental margins: where
850 shallow meets deep. Trends Ecol. Evol. *24*, 606-617.

851 Levin, L.A. 2006. Recent progress in understanding larval dispersal: New directions and
852 digressions. Int. Comp. Biol. 46:282-297.

853 Levin. LA, R.J. Etter, MA Rex, AJ Gooday, CR Smith, J Pineda, CT Stuart, RR Hessler,
854 and D Pawson. 2001 Environmental influences on regional deep-sea species
855 diversity. Ann. Rev. Ecol. Evol. Syst. 32: 51-93.

856 Levitus, S., Antonov, J., Boyer, T.P., 1994a. Interannual variability of temperature at 125
857 m depth in the North Atlantic Ocean. Science 266, 96–99.

858 Levitus, S., Boyer, T.P., & Antonov, J. 1994b. World Ocean Atlas, vol. 4, Temperature
859 NOAA Atlas NESDIS 4. Washington D.C.: U.S. Government Printing Office, p. 117.

860 Lippold, J., Luo, Y., Francois, R., Allen, S.E., Gherardi, J., Pichat, S., Hickey, B., Schulz,
861 H., 2012. Strength and geometry of the glacial Atlantic Meridional Overturning
862 Circulation. Nat. Geosci. 5, 813–816.

863 López-Duarte, P. C., Carson, H. S., Cook, G. S., Fodrie, F. J., Becker, B. J., DiBacco, C.,
864 & Levin, L. A. 2012. What controls connectivity? An empirical, multi-species
865 approach. Integr. Comp. Biol., *52*, 511-524.

866 Lowe, W. H., Allendorf, F. W. 2010. What can genetics tell us about population
867 connectivity? Mol. Ecol. *19*, 3038-3051.

868 Lozier, M. S., Gary, S. F., & Bower, A. S. 2013. Simulated pathways of the overflow
869 waters in the North Atlantic: Subpolar to subtropical export. Deep-Sea Res. II *85*,
870 147-153.

871 Marsh, A. G., Mullineaux, L. S., Young, C. M., Manahan, D. T. 2001. Larval dispersal
872 potential of the tubeworm Riftia pachyptila at deep-sea hydrothermal vents. Nature,
873 *411*, 77-80.

874 Marshall DJ, Monro K, Bode M, Keough MJ, Swearer S 2010 Phenotype-environment
875 mismatches reduce connectivity in the sea. Ecol Lett 13: 128–140.
876 doi:10.1111/j.1461-0248.2009.01408.x. PubMed: 19968695.

877 McGillicuddy Jr, D. J., Lavelle, J. W., Thurnherr, A. M., Kosnyrev, V. K., Mullineaux, L.
878 S. 2010. Larval dispersion along an axially symmetric mid-ocean ridge. Deep-Sea
879 Res. I *57*, 880-892.

880 McManus, J.F., Francois, R., Gherardi, J.-M., Keigwin, L.D., Brown-Leger, S., 2004.
881 Collapse and rapid resumption of Atlantic meridional circulation linked to deglacial
882 climate changes. Nature 428, 834–837.

883 Mengerink KJ, Van Dover CL, Ardron J, Baker M, Escobar-Briones E, Gjerde K,
884 Koslow JA, Ramirez-Llodra E, Lara-Lopez A, Squires D, Sutton T, Sweetman AK,
885 Levin LA. 2014. A call for deep-ocean stewardship. Science 344: 696–698.

886 Mitarai S, Siegel DA, Watson JR, Dong C, McWilliams JC 2009. Quantifying
887 connectivity in the coastal ocean with application to the Southern California Bight. J
888 Geophys Res, C10026, doi:10.1029/2008JC005166

889 Morgan, S.G. 2014. Behaviorally mediated larval transport in upwelling systems.
890 Advances in Oceanography vol. 2014, Article ID 364214, 17 pages, 2014.
891 doi:10.1155/2014/364214

892 Mouquet N., M. Loreau. 2003. Community patterns in source-sink metacommunities.
893 Am. Nat. 162, 544-557.

894 Mullineaux, L. S., McGillicuddy Jr, D. J., Mills, S. W., Kosnyrev, V. K., Thurnherr, A.
895 M., Ledwell, J. R., & Lavelle, J. W. 2013. Active positioning of vent larvae at a mid-
896 ocean ridge. Deep-Sea Res. II *92*, 46-57.

897 Mullineaux, L.S., Adams, D.K., Mills, S.W., Beaulieu, S.E., 2010. Larvae from afar
898 colonize deep-sea hydrothermal vents after a catastrophic eruption. Proc. Natl. Acad.
899 Sci., *107*, 7829-7834

900 Mullineaux, L.S., Speer, K.G., Thurnherr, A.M., Maltrud, M.E., Vangriesheim, A., 2002.
901 Implications of cross-axis flow for larval dispersal along mid-ocean ridges. Cahiers
902 de Biologie Marine 43, 281–284.

903 Nathan, R. 2006. Long-distance dispersal of plants. Science, *313*, 786-788.

904 Neubert, M. G., Caswell, H. 2000. Demography and dispersal: calculation and sensitivity
905 analysis of invasion speed for structured populations. Ecology, *81*, 1613-1628.

906 North, E. W., Schlag, Z., Hood, R. R., Li, M., Zhong, L., Gross, T., & Kennedy, V. S.
907 2008. Vertical swimming behavior influences the dispersal of simulated oyster larvae
908 in a coupled particle-tracking and hydrodynamic model of Chesapeake Bay. Mar.
909 Ecol. Prog. Ser. 359:99-115.

910 Nosil, P. 2012. Ecological Speciation. 280 pp. Oxford University Press.

911 Nosil, P., Vines, T. H., Funk, D. J. 2005. Perspective: Reproductive isolation caused by
912 natural selection against immigrants from divergent habitats. Evolution 59:705–719.

913 O'Connor, M. I., Bruno, J. F., Gaines, S. D., Halpern, B. S., Lester, S. E., Kinlan, B. P.,
914 Weiss, J. M. 2007. Temperature control of larval dispersal and the implications for
915 marine ecology, evolution, and conservation. Proc. Natl. Acad. Sci. *104*, 1266-1271.

916 Pacanowski, R.C., 1996. MOM 2 Documentation User's Guide and Reference Manual.
917 NJ: GFDL/NOAA, Princeton.

918 Palumbi, S.R. 2003. Population genetics, demographic connectivity, and the design of
919 marine reserves. Ecol. Appl. 13:146-158.

920 Paris, C.B., Cherubin, L.M., Cowen, R.K. 2007. Surfing, spinning, or diving from reef to
921 reef: effects on population connectivity. Mar. Ecol. Prog. Ser. 347:285-300.

922 Peck, L. S., Powell, D. K., Tyler, P. A. 2007. Very slow development in two Antarctic
923 bivalve molluscs, the infaunal clam *Laternula elliptica* and the scallop *Adamussium*
924 *colbecki*. Mar. Biol. 150, 1191-1197.

925 Pickart, R.S., Watts, D.R., 1990. Deep Western Boundary Current variability at Cape
926 Hatteras. J. Mar. Res. 48, 765–791.

927 Pusceddu, A., Bianchelli, S., Martín, J., Puig, P., Palanques, A., Masqué, P., Danovaro,
928 R. 2014. Chronic and intensive bottom trawling impairs deep-sea biodiversity and
929 ecosystem functioning. Proc. Natl. Acad. Sci. *111*, 8861-8866.

930 Quattrini AM, Georgian SE, Byrnes L, Stevens A, Falco R, Cordes EE. 2013 Niche
931 divergence by deep-sea octocorals in the genus *Callogorgia* across the continental
932 slope of the Gulf of Mexico. Mol. Ecol. 22**,** 4123-4140.

933 Ramirez-Llodra E, Tyler PA, Baker MC, Bergstad OA, Clark MR, Escobar E, Levin LA,
934 Menot L, Rowden AA, Smith CR, Van Dover CL. 2011. Man and the last great
935 wilderness: human impact on the deep sea. *PLoS ONE* 6: e22588.

936 Rex MA. 1981. Community structure in the deep-sea benthos. Ann. Rev. Ecol. Evol.
937 Syst. 12: 331–353.

938 Rex, M.A. and R.J. Etter. 2010. *Deep-Sea Biodiversity: Pattern and Scale*. 354 pp.

939 Harvard University Press.

940 Rhein, M., Weiss, R.F., Mertens, C., Min, D.H., Fleischmann, U., Putzka, A., Fischer, J.,
941 Smethie, W.M., Smythe-Wright, D., 2002. Labrador Sea Water: pathways, CFC
942 inventory, and formation rates. J. Phys. Oceanogr. 32, 648–665.

943 Riginos, C., Buckley, Y. M., Blomberg, S. P., Treml, E. A. 2014. Dispersal capacity
944 predicts both population genetic structure and species richness in reef fishes. Am.
945 Nat. 184, 52-64.

946 Roughgarden, J., Iwasa, Y., Baxter, C. 1985. Demographic theory for an open marine
947 population with space-limited recruitment. Ecology, 66, 54-67.
948
949 Sakina-Dorothée, A., Lazure, P., Thiébaut, É. 2010. How does the connectivity between
950 populations mediate range limits of marine invertebrates? A case study of larval
951 dispersal between the Bay of Biscay and the English Channel (North-East Atlantic).
952 Progr. Oceanogr. 87, 18-36.

953 Sala, I., Caldeira, R. M., Estrada-Allis, S. N., Froufe, E., Couvelard, X. 2013. Lagrangian
954 transport pathways in the northeast Atlantic and their environmental impact. Limnol.
955 Oceanogr.: Fluids & Environments, *3*, 40-60.

956 Scheltema, R. S., Williams, I. P. 2009. Reproduction among protobranch bivalves of the
957 family Nuculidae from sublittoral, bathyal, and abyssal depths off the New England
958 coast of North America. Deep-Sea Res. II 56, 1835-1846.

959 Selkoe, K. Toonen, R.J. 2011. Marine connectivity: a new look at pelagic larval
960 duration and genetic metrics of dispersal. Mar. Ecol. Prog. Ser. 436, 291-305.

961 Shanks AL 2009. Pelagic larval duration and dispersal distance revisited. Biol. Bull. 216,
962 373–385.

963 Siegel, D. A., Mitarai, S., Costello, C. J., Gaines, S. D., Kendall, B. E., Warner, R. R., &
964 Winters, K. B. 2008. The stochastic nature of larval connectivity among nearshore
965 marine populations. Proc. Natl. Acad. Sci. USA 105:8974-8979.

966 Somero GN. 1992. Adaptations to high hydrostatic pressure. Ann. Rev. Phys. 54, 557–
967 577.

968 Sotka, E. E., Wares, J. P., Barth, J. A., Grosberg, R. K., Palumbi, S. 2004. Strong genetic
969 clines and geographical variation in gene flow in the rocky intertidal barnacle Balanus
970 glandula. Mol. Ecol. *13*, 2143-2156.

971 Sunday, J. M., Popovic, I., Palen, W. J., Foreman, M. G. G., & Hart, M. W. 2014. Ocean
972 circulation model predicts high genetic structure observed in a long□lived pelagic
973 developer. Mol. Ecol. *23*, 5036-5047.

974 Thorrold, S.R., D.C. Zacherl, and L.A. Levin. 2007. Population connectivity and larval

975 dispersal: using geochemical signatures in calcified structures. Oceanography 20:80-
976 89.

977 Toole JM, Curry RG, Joyce TM, McCartney M, Peña-Molino B. 2011. Transport of the
978 North Atlantic Deep Western Boundary Current about 39°N, 70°W: 2004– 2008.
979 Deep-Sea Res. II 58, 1768–1780.

980 Trakhtenbrot, A., Nathan, R., Perry, G., Richardson, D. M. 2005. The importance of
981 long□distance dispersal in biodiversity conservation. *Div. Distrib. 11*, 173-181.

982 Treml, E. A., Roberts, J. J., Chao, Y., Halpin, P. N., Possingham, H. P., Riginos, C.
983 2012. Reproductive output and duration of the pelagic larval stage determine
984 seascape-wide connectivity of marine populations. Integr. Comp. Biol. *52*, 525-537.

985 Tyler, P. A., Campos-Creasy, L. S., & Giles, L. A. 1994. Environmental control of quasi-
986 continuous and seasonal reproduction in deep-sea benthic invertebrates.
987 *Reproduction, larval biology, and recruitment of the deep-sea benthos. Columbia*
988 *University Press, New York*, 158-178.

989 van Sebille, E., P.J. v. Leeuwen, A. Biastoch, C.N. Barron, W.P.M. De Ruijter,
990 2009. Lagrangian validation of numerical drifter trajectories using drifting buoys:
991 aspplication to the Agulhas region. Ocean Modelling, 29, 269–276

992 Watling, L., Guinotte, J., Clark, M. R., & Smith, C. R. 2013. A proposed biogeography of
993 the deep ocean floor. Prog. Oceanogr., *111*, 91-112.

994 Watson, J. R., Mitarai, S., Siegel, D. A., Caselle, J. E., Dong, C., McWilliams, J. C. 2010.
995 Realized and potential larval connectivity in the Southern California Bight. Mar.
996 Prog. Ecol. Ser. *401*, 31-48.

997 Weersing K, Toonen RJ 2009 Population genetics, larval dispersal, and connectivity in
998 marine systems. Mar. Ecol. Prog. Ser. 393:1–12

999 White, C., Selkoe, K. A., Watson, J., Siegel, D. A., Zacherl, D. C., & Toonen, R. J. 2010.
1000 Ocean currents help explain population genetic structure. Proc. R. Soc. B 277, 1685-
1001 1694

1002 White, J. W., Morgan, S. G., Fisher, J. L. 2014. Planktonic larval mortality rates are
1003 lower than widely expected. Ecology. *95*, 3344-3353.

1004 Xue, H., Incze, L., Xu, D., Wolff, N., Pettigrew, N. 2008. Connectivity of lobster
1005 populations in the coastal Gulf of Maine Part I: Circulation and larval transport
1006 potential. Ecol. Model. 210:193-211.

1007 Yearsley JM, Sigwart JD 2011 Larval Transport Modeling of Deep-Sea Invertebrates
1008 Can Aid the Search for Undiscovered Populations. PLoS ONE 6(8): e23063.
1009 doi:10.1371/journal.pone.0023063

Young CM, Ekaratne SUK, Cameron JL. 1998. Thermal tolerances of embryos and planktotrophic larvae of *Archaeopneustes hystrix* (Spatangoidea) and *Stylocidaris lineata* (Cidaroidea), bathyal echinoids from the Bahamian Slope. J. Exp. Mar. Biol. Ecol. 223:65–76.

Young CM, Tyler PA 1993 Embryos of the deep-sea echinoid Echinus affinis require high pressure for development. Limnol. Oceanogr. 38, 178–181.

Young CM, Tyler PA, Gage JD 1996 Vertical distribution correlates with pressure tolerances of early embryos in the deep-sea asteroid *Plutonaster bifrons*. J. Mar. Biol. Ass. UK, 76, 749–757.

Young, C. M., He, R., Emlet, R. B., Li, Y., Qian, H., Arellano, S. M., Van Gaest, A., Bennett, K.C., Wolf, M., Smart, T.I., Rice, M. E. 2012. Dispersal of deep-sea larvae from the Intra-American Seas: simulations of trajectories using ocean models. Integr. Comp. Biol. *52*, 483-496.

Zardus JD 2002 Protobranch bivalves. Adv. Mar. Biol. 42, 1–65.

Zardus, J. D., Etter, R. J., Chase, M. R., Rex, M. A., Boyle, E. E. 2006. Bathymetric and geographic population structure in the pan-Atlantic deep-sea bivalve *Deminucula atacellana* (Schenck 1939). Mol. Ecol. 15. 639-651.

1031 Table 1: Percentage of particles that are located offshore of release depth (i.e., in
1032 deeper water) as a function of release depth and time.
1033

Release Depth (m)	30 days	180 days	360 days	1500 days
1500	81	98	99	100
2000	90	92	98	98
2500	51	79	83	98
3200	38	55	68	92

1034
1035

Figure Legends

Figure 1. a) Map of the locations where previous genetic work was conducted (squares) with station numbers given next to each box and the locations where simulated trajectories were initiated for Lagrangian estimates of dispersal and connectivity (circles). The solid dark rectangle indicates the location of the Line W moored array (Toole et al. 2011). DWBC and Gulf Stream paths are illustrated schematically by blue and red block arrows, respectively. Isobaths are shown every 500 m. Note that the main genetic breaks in protobranch bivalves occurred between stations 9 and 14. b) Multilocus phylogenetic relationships among individuals from shallow (stations 4, 5, 6, 7, and 9) and deep (10, 17, 18) stations for *Deminucula atacellana* based on five loci (from Jennings et al. 2013). c) Multilocus phylogenetic relationships among individuals from shallow (6, 7, and 10) and deep (14, 17, 18) stations for *Neilonella salicensis* based on three loci (from Glazier and Etter 2014).

Figure 2. (a) Section of time mean current speed perpendicular to the Line W section from 15-year run of FLAME. Circled black dots indicate model grid points where simulated trajectories were initiated. (b) Measured flows derived from the Line W array (From Toole et al. 2011; current meters are indicated by black dots, temperature/conductivity meters are indicated by green dots) across the same transect in (a). Velocity is color coded with negative values indicating southwestern flow and positive values northeastern flow. The similarity indicates that the major flow features are well characterized in the circulation model.

1060 Figure 3. Ten sample trajectories of neutrally buoyant particles released at 1500 m (a),
1061 2000 m (b), 2500 m (c) and 3200 m (d) depth in the western North Atlantic. The open
1062 circle indicates the release point. Trajectories are color-coded based on time since
1063 release: 0-30 days – red, 31-180 days – green, 181-360 days – blue. Isobaths every
1064 1000m are color-coded black, cyan, yellow, and brown respectively.
1065
1066 Figure 4. Potential connectivity maps of 360 particles after 30 days for different release
1067 depths in the DWBC. The shading indicates the number of particle visits at a specific
1068 model grid point (defined by a box with the same resolution as the model, 1/12º x 1/12º)
1069 during the first 30 days after release. The warmer the color, the more particles visited that
1070 grid box. The position of each particle at 30 days after release is shown as an orange dot
1071 (note that panel axes were chosen so that the structure of the contours was clear, which
1072 meant that some orange end point dots fell outside the panel axes). A circle with an X
1073 indicates the release point. Open circles depict the other three release points used in the
1074 study. Isobaths are depicted by thin black lines every 1000m.
1075
1076 Figure 5. Potential connectivity maps for different depths of release after 180 days.
1077 Details and color codes as described in Fig. 4.
1078
1079 Figure 6. Potential connectivity maps for different depths of release after 360 days.
1080 Details and color codes as described in Fig. 4.
1081

1082 Figure 7. Potential connectivity maps for different depths of release after 1500 days.
1083 Details and color codes as described in Fig. 4.
1084
1085 Figure 8. Particle displacement distributions. The distance of particles from their release
1086 point (measured as a straight-line distance) after 30, 180, 360 or 1500 days. The lines
1087 indicate the number of particles at different distances from their release point and are
1088 color-coded based on release depth. Inset bar graphs indicate the mean and standard
1089 error (colored bars with blue error bars) and median (black lines) displacement of
1090 particles after a specific number of days as a function of release depth. (dst = distance).
1091
1092
1093
1094
1095
1096

All Figures

Click here to download Figure: EtterBowerFigures.pdf

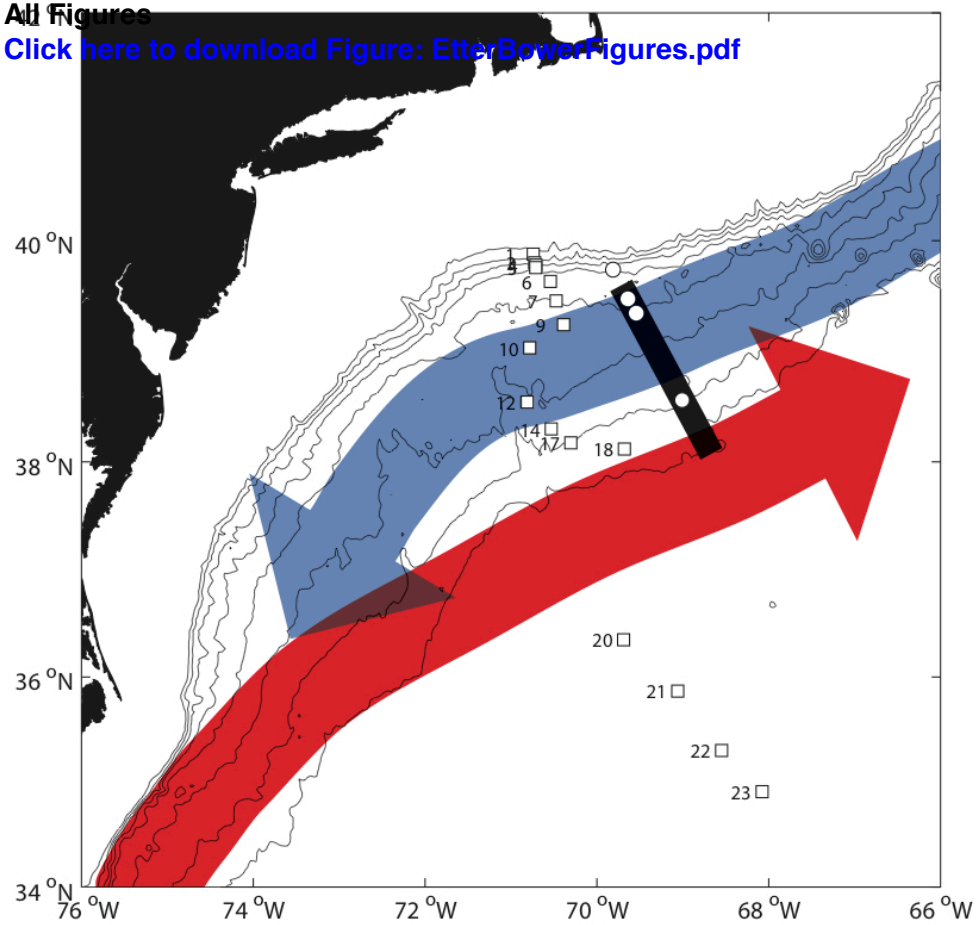

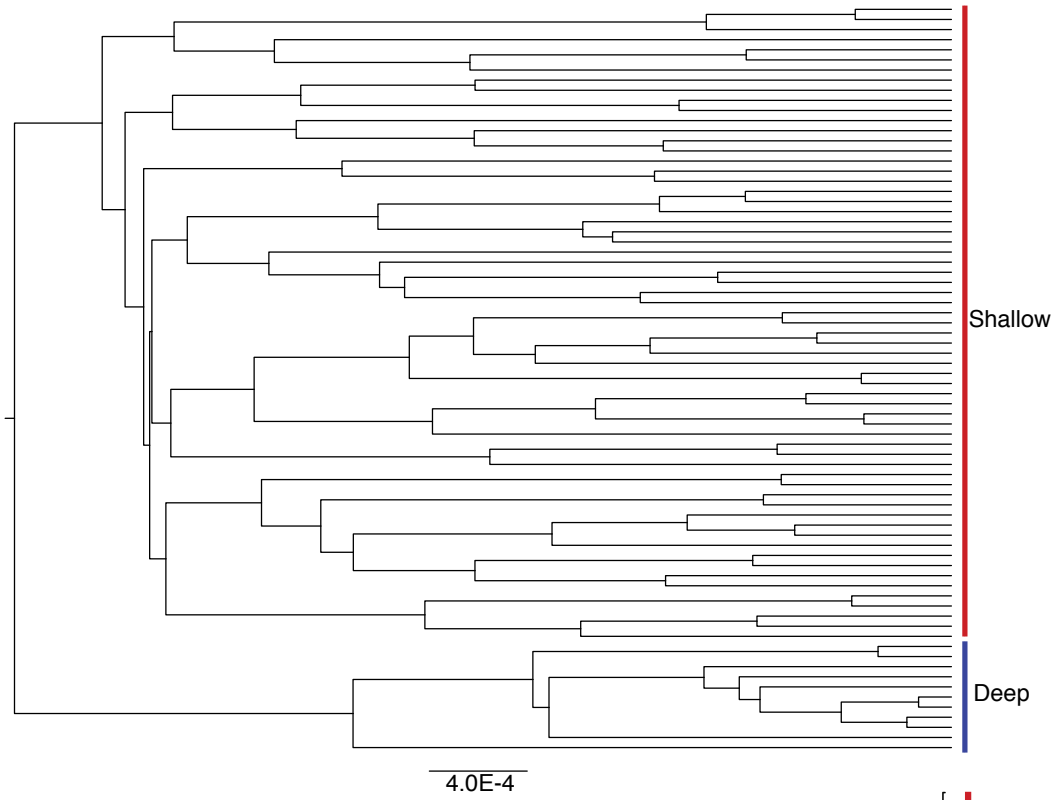

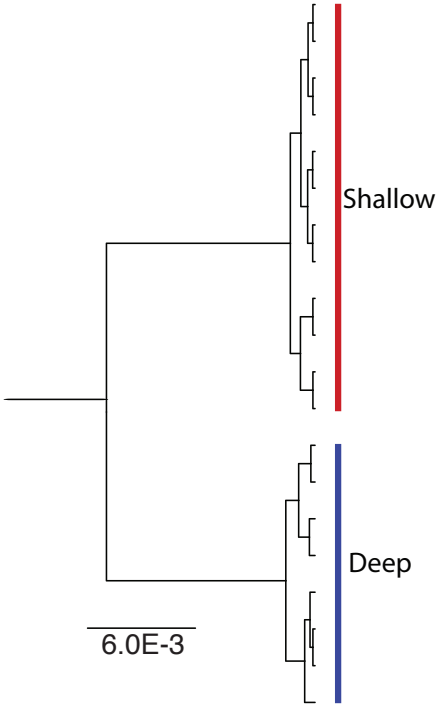

Figure 1.

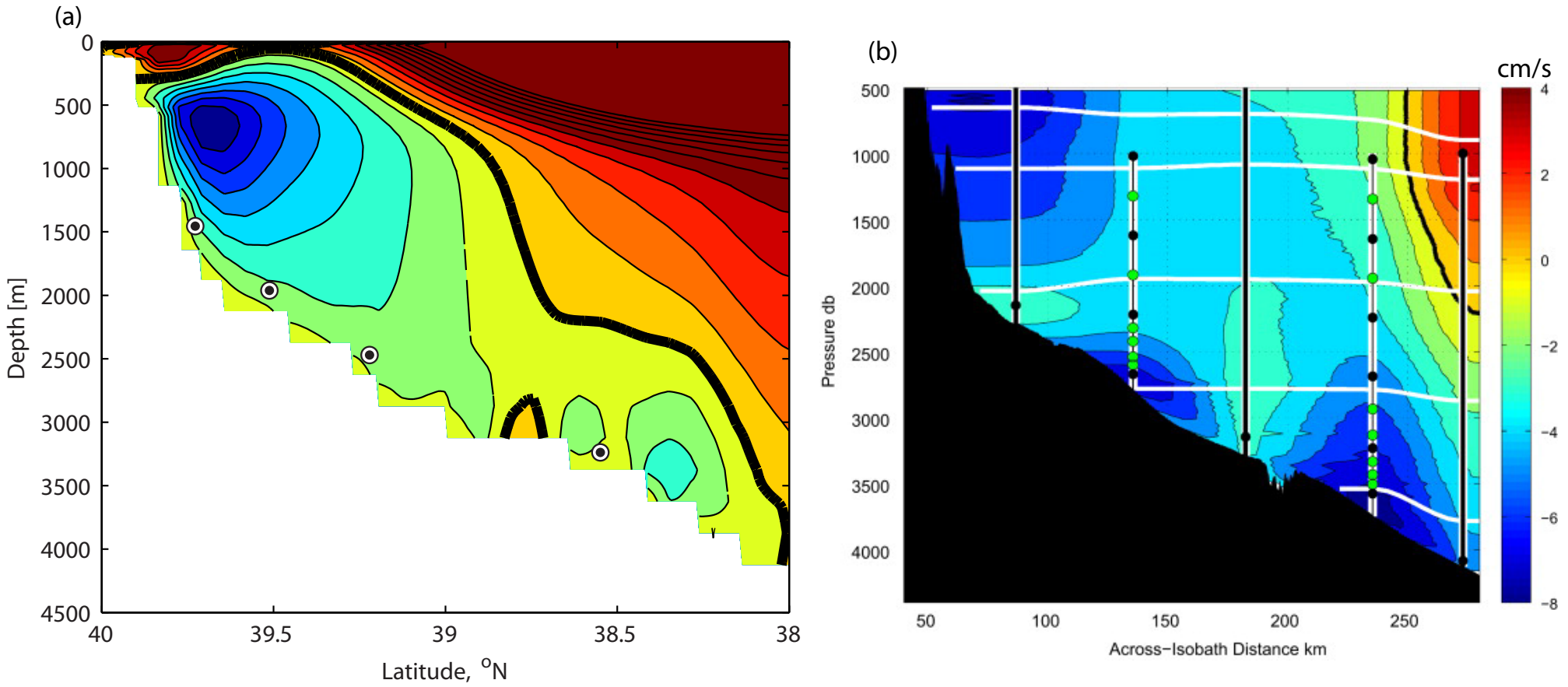
(a)
Depth [m]
0
500
1000
1500
2000
2500
3000
3500
4000
4500
40
39.5
39
38.5
38
Latitude, °N
(b)
cm/s
Pressure db
500
1000
1500
2000
2500
3000
3500
4000
50
100
150
200
250
Across−Isobath Distance km
4
2
0
−2
−4
−6
−8

Figure 2

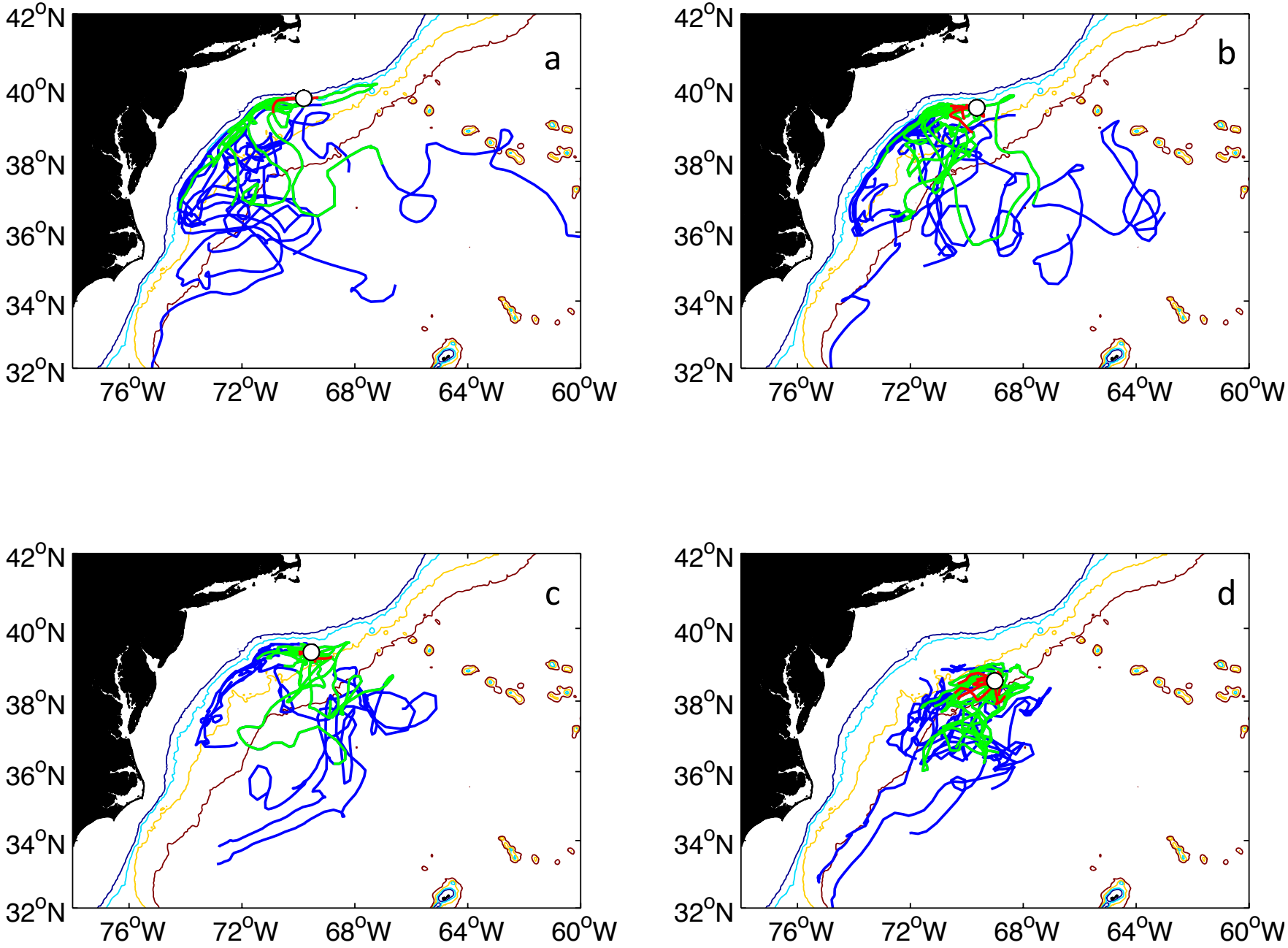

Figure 3

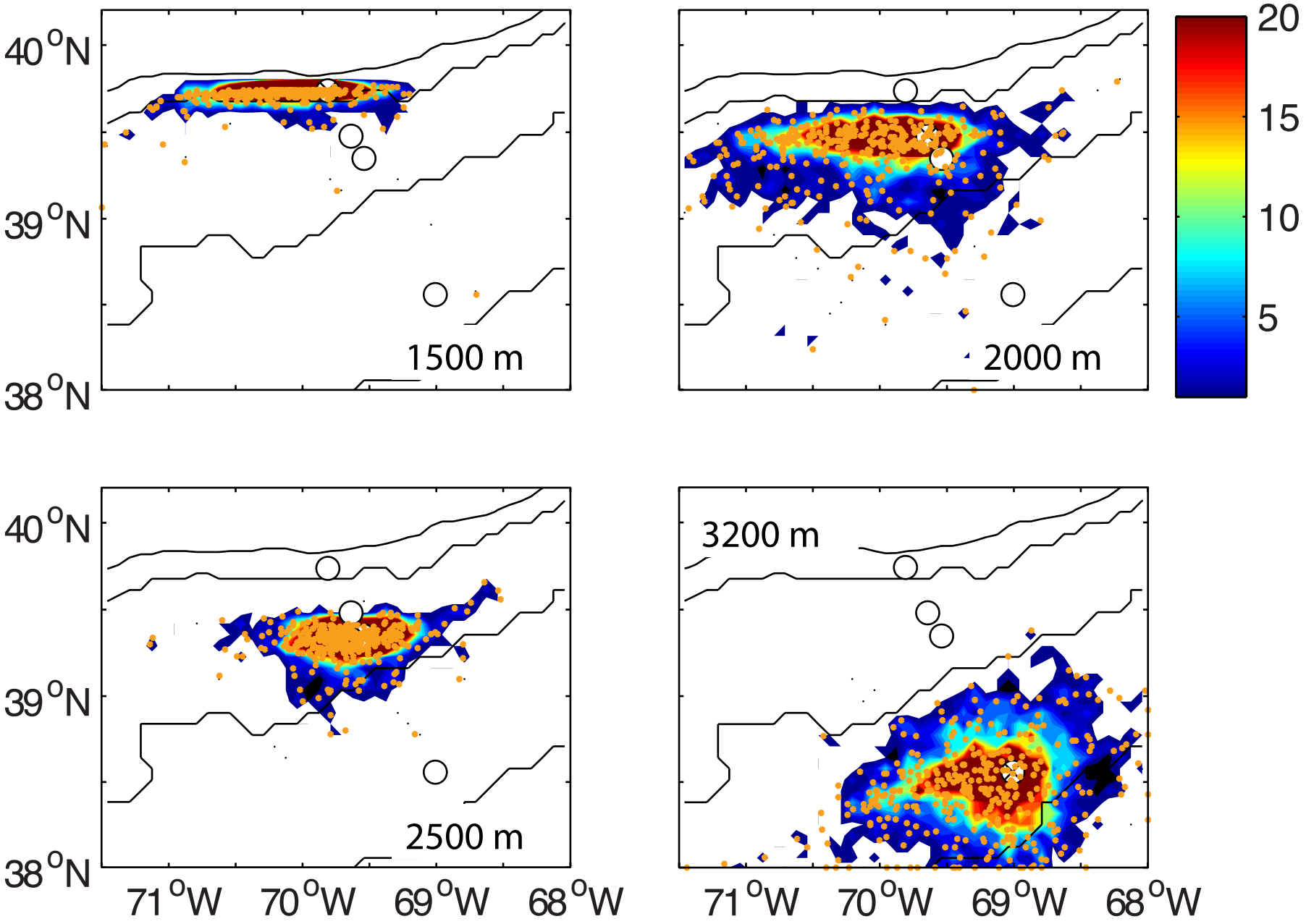

Figure 4.

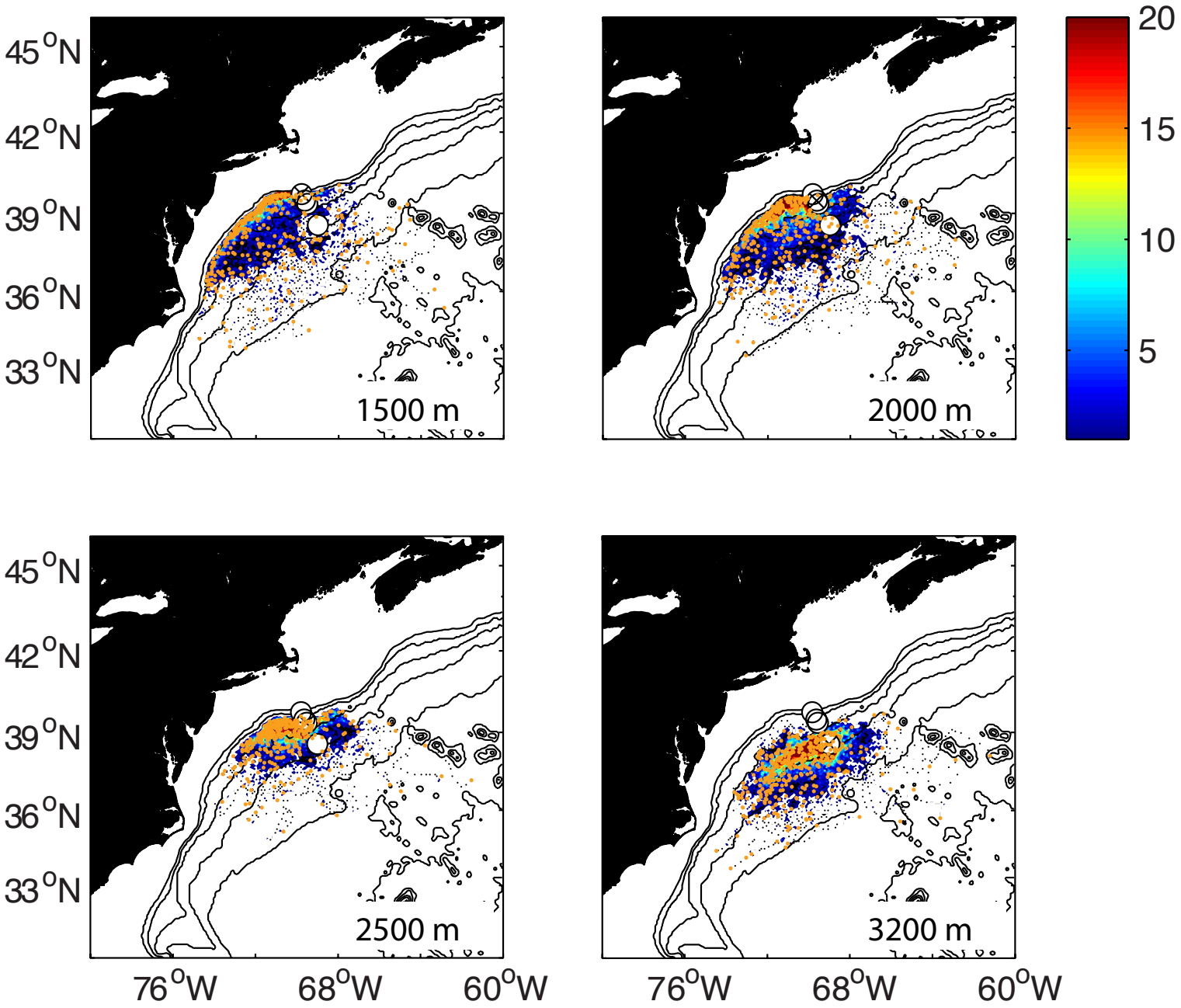
45°N
42°N
39°N
36°N
33°N
1500 m
2000 m
2500 m
3200 m
76°W
68°W
60°W
20
15
10
5

Figure 5.

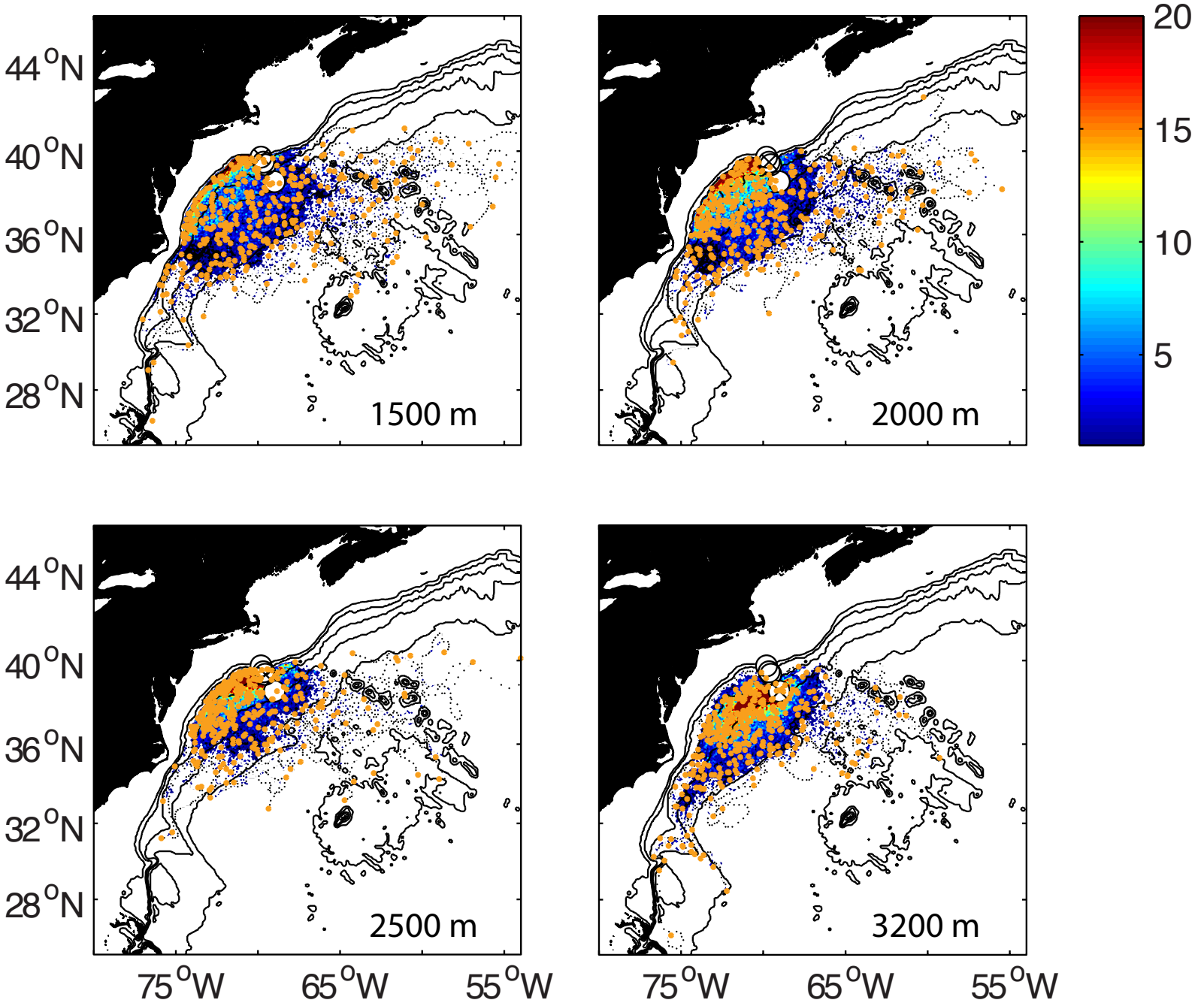
44°N
40°N
36°N
32°N
28°N
1500 m
2000 m
2500 m
3200 m
75°W
65°W
55°W
20
15
10
5

Figure 6.

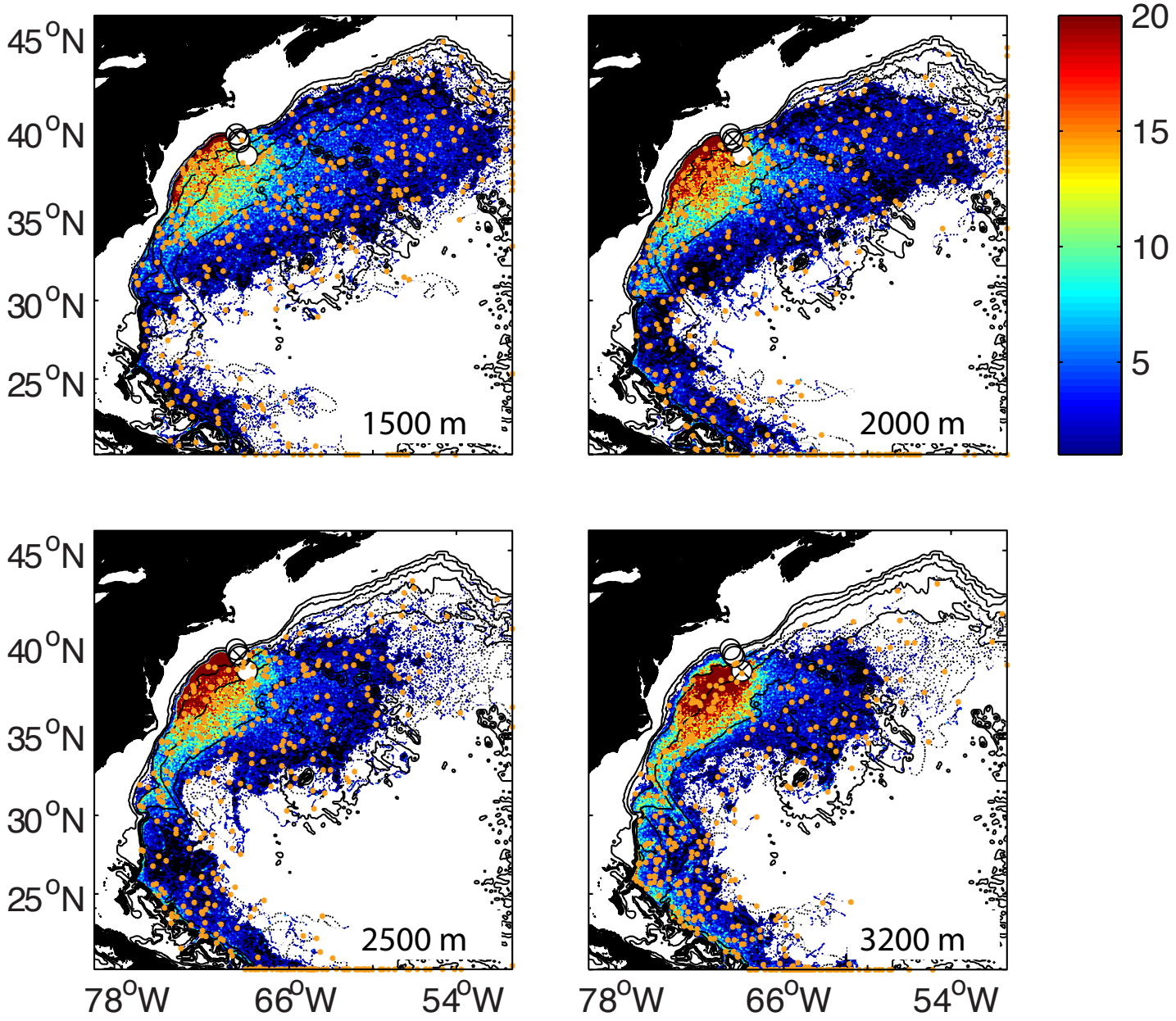
45°N
40°N
35°N
30°N
25°N
1500 m
2000 m
2500 m
3200 m
78°W
66°W
54°W
20
15
10
5

Figure 7

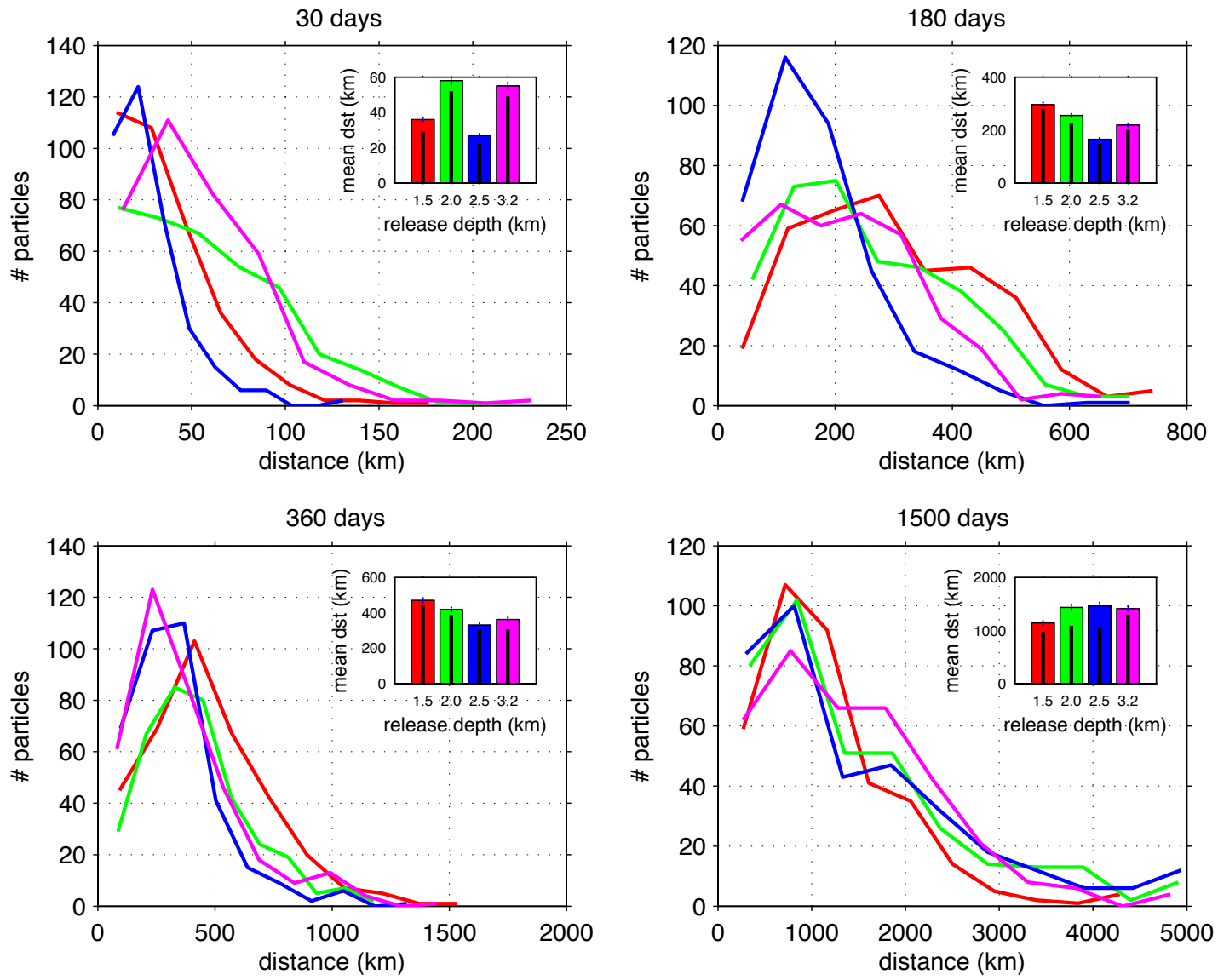
30 days
180 days
360 days
1500 days
particles
distance (km)
mean dst (km)
release depth (km)
1.5 2.0 2.5 3.2

Figure 8